School of Medicine
Oregon Health & Science University

CERTIFICATE OF APPROVAL

This is to certify that the Ph.D. dissertation of

Catherine Selph

has been approved

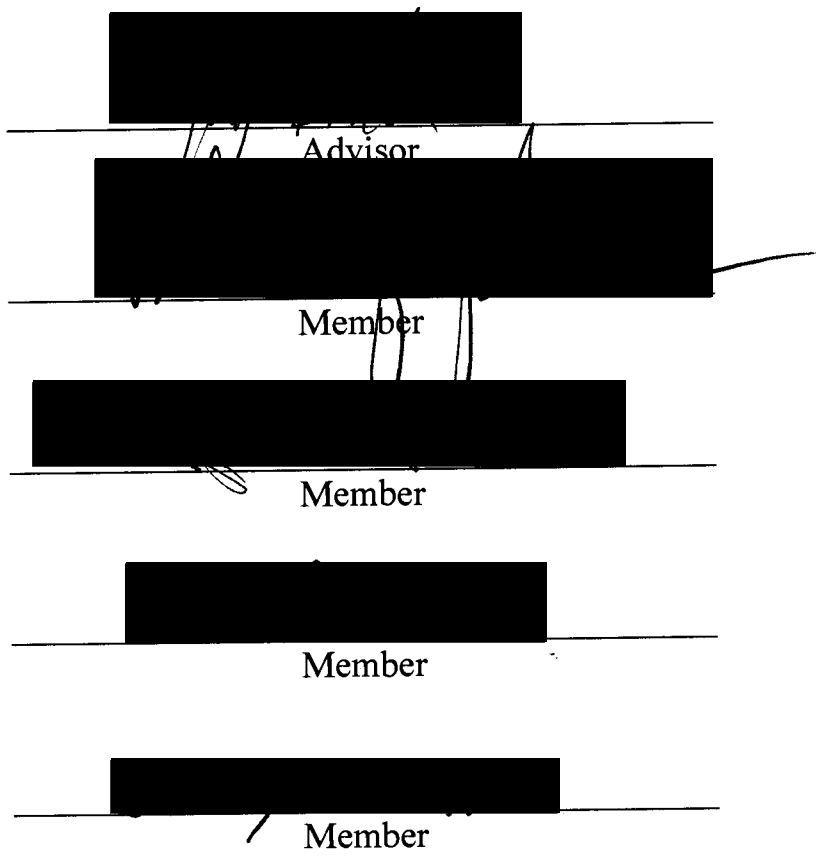

The Selective Translocation of the Molecular Motor Kinesin-1 during the Development of Neuronal Polarity in Culture

by Catherine Selph

A Dissertation

Presented to the Department of Physiology and Pharmacology
and the Oregon Health & Science University School of Medicine

in partial fulfillment of
the requirements for the Degree of
Doctor of Philosophy

May 2006

Table of Contents

List of Figures

Movies 1-9 are on the included CD.

Chapter 4

Movies 1-12 are on the included CD.

List of Tables

List of Abbreviations

APP	Amyloid Precursor Protein
ATP	Adenosine Triphosphate
ATPase	Adenosine Triphosphatase
CHO	Chinese Hamster Ovary
CLIP170	Cytoplasmic Linker Protein 170
EB1	End-binding Protein 1
FIONA	Fluorescence Imaging One-Nanometer Accuracy
GABA	Gamma-aminobutyric Acid
GFP	Green Fluorescent Protein
GST	Glutathione S-transferase
KHC	Kinesin Heavy Chain
Kif1A	Kinesin Family Member 1A
Kif5C	Kinesin Family Member 5C
KLC	Kinesin Light Chain
MAP	Microtubule-associated Protein
mRNA	Messenger Ribonucleic Acid
MTOC	Microtubule Organizing Center
NgCAM	Neuronal-glial Cell Adhesion Molecule
PA-GFP	Photo-activatable Green Fluorescent Protein
PtdIns(4,5)P2	Phosphatidylinositol(4,5)bisphosphate
PTM	Post-translational Modification
STOP	Stable Tubule Only Polypeptide
SV2	Synaptic Vesicle Protein 2
TGN	*trans*-Golgi Network
TIRF	Total Internal Reflection Microscopy
TPR	Tetratrico Repeat

Acknowledgements

Thanks to my wonderful husband Aaron for being my rock through all of the ups and downs of the long hike through graduate school. Thanks to my ever-supportive parents Ann and Rich who got me to graduate school in the first place. Without you this would not have been possible. Thanks to my siblings Elizabeth, Brac and David for always being there to cheer me up and keep me going. Thanks to Gary for inviting me into his lab to do my graduate work, and for teaching me that science happens within an historical context. Thanks to Stefanie, our everywoman-in-one lab manager and imaging director extraordinaire. Thanks to my support system of old and new friends who each came through for me with love and encouragement at various times in my life.

Abstract

To establish and maintain the functional differences between axons and dendrites, neurons must transport distinct sets of proteins to each compartment. This long-range intracellular transport occurs via a network of microtubule "tracks", along which the molecular motors kinesin and dynein translocate, using energy derived from ATP hydrolysis. How this transport system is organized to ensure the delivery of specific cargo to precise destinations is still largely unknown. This dissertation concerns the role that kinesin motor proteins might play in specifying the destination of cargo. Specifically, this work examines whether individual kinesins preferentially translocate along a particular subset of microtubules directed toward specific subcellular destinations in cultured hippocampal neurons.

The accumulation of constitutively active, fluorescently tagged kinesin motors was used as a measure of where they translocate. In particular, the focus was on two well-studied kinesins that are known to play important roles in cargo transport in neurons. Constitutively active Kif1A (a Kinesin-3 family member) accumulated at the tips of all neurites. In contrast, constitutively active Kif5C (a Kinesin-1 family member) accumulated selectively in axons. Taxol treatment abolished the selectivity of Kif5C. Taxol treatment also reduced microtubule dynamics. However, distinct microtubule dynamics were not a good predictor of Kif5C localization.

Before neurons became polarized, constitutively active Kif1A accumulated in all neurites, consistent with its behavior at later stages of

development. Unexpectedly, constitutively active Kif5C transiently accumulated in one neurite at a time. Coincident with axon specification, constitutively active Kif5C accumulated only in the emerging axon and no longer appeared in any other neurite. These findings suggest that the translocation of Kif5C along a biochemically distinct track leading to the nascent axon could ensure the selective delivery of Kif5C cargoes to the axon and hence contribute to its molecular specification. Moreover, this work identified a novel molecular marker that can be used to study the development of neuronal polarity in living neurons. Imaging YFP-tagged constitutively active Kif5C provides the most precise definition to date of when neuronal polarity first emerges and allows visualization of the molecular differentiation of the axon in real time.

Chapter 1: Introduction to the Dissertation

Organization of Transport in Neurons: Open Questions

While all eukaryotic cells need a transport system to distribute cargoes within the cell, neurons require one with a particularly high degree of spatial and temporal organization. Neurons are highly polarized cells that develop and maintain two morphologically and functionally distinct domains, the axon and the dendrites. Proteins are synthesized in the cell body and must then be transported to specific subdomains throughout the neuron, sometimes at great distances from their site of synthesis. This long-range intracellular transport occurs via a network of microtubule "tracks", along which the molecular motors kinesin and dynein translocate, using energy derived from ATP hydrolysis.

How this transport system is organized to ensure the delivery of specific cargo to precise destinations is still largely unknown. First, there is the question of whether cargo-motor interactions are specific. The highly divergent cargo binding domains of different kinesin family members have led to the hypothesis that specific kinesins only transport particular cargoes (Karcher et al., 2002). However, there must also be redundancy among motors because the number of cargoes is far greater than the number of kinesins that have been identified. Second, there is the question of which pathway the motor-cargo complex chooses to move along. Microtubules are intrinsically polarized, with defined plus and minus ends (Desai & Mitchison, 1997). Since kinesins are known to be directional (Vale, 2003), the pathway of a particular motor-cargo complex is, in part, determined by the polarity orientation of the microtubules. In mature

neurons, for example, microtubules in the axon are oriented with their plus ends distal (Baas et al, 1989), which would preclude a minus end-directed motor from transporting cargo in the anterograde direction in that process. There is also evidence that kinesins distinguish more than the mere directionality of microtubules, which could lead to the preferential transport of their cargo to a particular subcellular destination. Finally, cargo must dissociate from its motor at the appropriate destination. *In vitro* studies suggest that this process is regulated by signaling proteins, such as kinases and heat shock proteins (Tsai et al., 2000), leading to the hypothesis that cytosolic factors present at the cargo's destination release the cargo from the motor. This dissertation concerns the second question: do specific kinesins translocate preferentially along microtubules leading to the axon or to the dendrites? Such preferential translocation would imply that there are subsets of microtubules that are molecularly modified such that a kinesin might distinguish them from other microtubules, and thereby have a preferred pathway for transporting its cargo within the neuron.

Experimental Approach

One way to determine whether kinesins can distinguish between distinct populations of microtubules in a cell is to ask where a constitutively active version accumulates. In this approach the localization of constitutively active kinesins is used as a measure of where they translocate. Cultured hippocampal neurons are particularly well-suited to this approach. At a certain developmental stage, before the dendrites have matured, microtubules in all neurites are oriented

in the same way; both axons and dendrites contain primarily plus end out microtubules (Baas et al, 1989). Thus, a constitutively active plus end-directed motor would be expected to accumulate at the ends of all neurites. In contrast, the preferential translocation of the motor in one domain could be revealed by its *selective* accumulation at the tips of either the axon or the dendrites.

I used this approach to visualize the subcellular localization of two well-studied kinesins, Kif1A (a Kinesin-3 family member) and Kif5C (a Kinesin-1 family member). Constitutively active versions of these two kinesins contain the minimal domains necessary for a functional motor, including the catalytic motor domains that hydrolyze ATP and bind to microtubules, and important dimerization domains. However, the tails, which contain the cargo-binding domains as well as the regulatory domains responsible for the inactivation of the motors, have been removed. *In vitro* and *in vivo* studies have shown that such a truncation results in a motor that continuously translocates along microtubules (Friedman & Vale, 1999, Tomishige et al, 2000, Nakata & Hirokawa, 2003, Lee et al, 2004). Thus, in a living cell, when such a constitutively active kinesin encounters a microtubule, it binds and translocates along that microtubule, until it dissociates with some probability and diffuses in the cytoplasm until its next encounter with a microtubule, at which point the cycle repeats itself. In this way, if the motor translocates non-selectively, it should accumulate where the plus ends of the microtubules ultimately end – in the case of stage 3 hippocampal neurons, at the ends of axons and dendrites. While I observed this pattern with some kinesins, my results show that other kinesins translocate preferentially in the

axon. This dissertation explores the mechanisms and implications of this fundamental observation.

Organization of the Dissertation

Chapter 2 of this dissertation provides a review of the important background literature that serves to ground the experimental work. In that chapter, I not only explain the current thinking on the regulation of kinesin motor proteins, but I also raise the question that this dissertation addresses.

Chapter 3 presents results of experiments concerning the localization of constitutively active kinesins in neurons. Briefly, I found that constitutively active Kif5C accumulates at the ends of the axons, but not dendrites, of cultured hippocampal neurons. In contrast, constitutively active Kif1A is not selective, and accumulates at the ends of both axons and dendrites. The selective localization of constitutively active Kif5C is completely dependent on its catalytic head domain, suggesting that this motor interacts differently with two distinct populations of microtubules in the neuron – those in the axon and those in dendrites. Furthermore, this result suggests that microtubule modifications affect the function of two kinesin motor proteins differently. This discovery was quite unexpected because the domain that interacts with microtubules (the catalytic head domain) is highly conserved among kinesin family members. It was difficult to imagine that two kinesins with such similar microtubule-interacting domains would exhibit different translocation patterns within a neuron.

To further understand the mechanism of the selectivity of constitutively active Kif5C, I examined the motor's distribution during axon specification using live cell imaging. Before axon specification, hippocampal neurons in culture are thought to be unpolarized. After plating, neurons initially sprout several seemingly identical neurites, which, by default, are thought to be pre-dendritic in character. These neurites intermittently grow and retract, until one stops retracting and continues to elongate, becoming the axon. It is thought that axon outgrowth is the first step to distinguish one neurite from the rest; the result being a polarized neuron. However, the time-lapse images of the distribution of constitutively active Kif5C during axon formation in Chapter 3 paint a different picture of axon specification. Constitutively active Kif5C selectively accumulates at the tip of a single neurite even before axon specification. This selective accumulation is transient, lasting between 15 minutes and two hours, and alternates between different neurites. Thus, neurites become temporarily differentiated well before the emergence of the axon. Furthermore, the motor domain of Kif5C spends as much time in other neurites as in the future axon, indicating that these transient molecular differentiations cannot predict axon identity.

I next looked for a correlation between molecular differentiation, as indicated by the selective accumulation of Kif5C in one neurite, and neurite growth, before axon specification. Surprisingly, these two events are not correlated, leading me to propose a new model for axon specification. This model holds that before axon specification, each neurite undergoes stochastic growth

events and, unrelated to these growth spurts, stochastic molecular differentiation events. When these two processes converge on the same neurite, that neurite has a high likelihood of becoming the axon.

The results presented in Chapter 3 laid the groundwork for the experiments described in Chapter 4. The findings in Chapter 3 indicate that Kif5C exhibits a preference for a subpopulation of microtubules. Thus, in Chapter 4, I focused on clarifying the mechanisms underlying the differential interaction of the motor with distinct types of microtubules. Axonal microtubules are thought to be more stable (Baas et al, 1991). Therefore, one possible explanation for the selective localization of Kif5C is that this motor prefers microtubules that are more stable. Consistent with this hypothesis, the selectivity of constitutively active Kif5 in *mature* hippocampal neurons is abolished by treatment with the microtubule-stabilizing drug taxol (Nakata & Hirokawa, 2003). These authors also found that Kif5 exhibits a higher affinity for microtubules in the initial segment of mature axons, and that taxol eliminates this difference in affinity. These studies suggest that microtubule dynamics may play a role in modulating the motor-microtubule interaction. However, Nakata and Hirokawa (2003) focused on the role of the initial segment which, as Chapter 3 will show, is not required for the selectivity of Kif5C. Therefore I examined the relationship between microtubule dynamics and Kif5C localization at earlier stages of development, both before and after axon specification.

I tested the effects of taxol on the accumulation of Kif5C. Using live cell imaging, I found that taxol abolishes the selective accumulation of Kif5C in a

manner consistent with its non-selective translocation in all neurites. This result suggests that taxol alters the modifications of the different microtubules such that they are now equal substrates for the motor. To confirm that taxol treatment stabilizes microtubules, I visualized the movements of EB1-GFP, a plus end tip binding protein that is used as a marker for microtubule polymerization dynamics (Vaughan, 2004, 2005). EB1-GFP movements are significantly reduced when the cells are treated with taxol.

The findings that taxol abolishes the selectivity of Kif5C and reduces microtubule dynamics led to the hypothesis that Kif5C localization correlates with reduced microtubule dynamics. To determine whether there was a correlation, I compared EB1 dynamics in Kif5C-positive neurites to EB1 dynamics in Kif5C-negative neurites. On average, there are slightly fewer EB1-GFP movements in Kif5C-positive neurites compared to Kif5C-negative neurites. However, there is no significant correlation between Kif5C localization and EB1-GFP dynamics, suggesting that microtubule dynamics are not a reliable predictor of Kif5C localization. The effects of taxol, therefore, cannot be explained by differences in microtubule dynamics alone. Rather, taxol must be having other indirect effects on post-translational modifications or microtubule-associated proteins, which in turn affect the motor's affinity for the microtubules.

In Chapter 5 I discuss the implications of the experimental observations presented in Chapters 3 and 4. In this chapter, I also consider experiments that will shed some light on the underlying molecular mechanisms of the selectivity of Kif5C as well as examine the physiological relevance of this selectivity.

Chapter 2: Review of the Literature

In this literature review, I cover topics that are relevant to the findings presented in Chapters 3 and 4. First, I introduce the Kinesin family of molecular motors. I focus on the two kinesins that are used in this dissertation – Kif5C in the Kinesin-1 family and Kif1A in the Kinesin-3 family. I discuss the structural basis for the regulation of the motors' activity as well as their mechanisms of motility. Next, I provide an summary of the experimental data that suggest that some cargoes are selectively transported in neurons. While this dissertation does not directly address cargo transport, the evidence for selective cargo transport suggests that the selective translocation of Kinesin-1 I observe is physiologically relevant. The subsequent section provides an overview of the microtubule cytoskeleton and discusses findings that are pertinent to the regulation of kinesins in neurons. Finally, I talk about the organization of the microtubule cytoskeleton during the development of hippocampal neurons in culture because it directly relates to the experimental approach that I used. In addition, I present the current model of how neurons develop polarity in culture and briefly discuss the relevance of the findings presented in this dissertation to this model.

Kinesin Motor Proteins

Overview

Kinesins are motor proteins that use the free energy derived from the hydrolysis of ATP to power movement along microtubules in a wide variety of cellular processes, including cell motility, cell division and organelle transport

(Goldstein & Yang, 2000, Vale, 2003). There are 14 known kinesin families, members of which have been discovered in every animal and plant cell studied (Lawrence et al., 2004). This number of kinesin families arose from a new classification scheme that was recently developed to address inconsistencies that emerged over the years due to the naming of kinesins by diverse criteria (Lawrence et al., 2004). Though kinesins were once believed to exclusively transport membrane organelles, it is now well documented that motors can move many other types of cargo, including protein complexes and complexes of nucleic acids with proteins (Goldstein, 2001, Karcher et al., 2002, Schnapp, 2003).

This review will focus on Kinesin-1 and Kinesin-3 family members. They comprise the major motors in cargo transport in neurons and are the subject of the experimental work discussed in this dissertation. Members of the Kinesin-1 and Kinesin-3 families have been linked to the transport of a variety of cargoes in neurons, including mRNA, mitochondria, lysosomes, synaptic vesicles, Golgi-derived carriers and endosomes (Vale, 2003).

In general, kinesin motor proteins contain a globular catalytic head domain at one end of a rod-shaped stalk and a cargo-binding domain at the other end (Vale & Fletterick, 1997). The head domain, which is highly conserved among all kinesin families, includes the microtubule binding and ATPase regions (Vale & Fletterick, 1997). The cargo-binding tails, on the other hand, are highly divergent among kinesin family members, and are thought to specify which cargo the motor transports (Vale & Fletterick, 1997, Goldstein & Philp, 1999). Though the regulatory mechanisms responsible for ensuring motor-cargo specificity are

still not fully known, it is generally thought that several different transport pathways move different classes of transport organelles following sorting in the cell body and association with specific motors (Goldstein, 2001, Karcher et al., 2002).

Kinesin-1: the First Kinesin to be Discovered

Kinesin-1, originally referred to as conventional kinesin, was first isolated in a biochemical fractionation of the squid giant axon for proteins that generate ATP-dependent microtubule-based motility *in vitro* (Schnapp et al., 1985, Vale et al., 1985a, Vale et al., 1985b). This discovery was facilitated by the development of video-enhanced differential interference contrast microscopy, a technique developed by Shinya Inoue and Robert Allen in the early 1980's that allowed structures below the resolution of the light microscope to be visualized and tracked in real time (Inoue 1981, Allen et al., 1982, Brady et al., 1982).

In vivo, the majority of Kinesin-1 exists in the cell as a soluble protein; only a small fraction is associated with its cargo at any given time (Hollenbeck, 1989). This property is a result of the inactivation of the non-cargo-bound motor (for discussion and references see *Tail Inhibition* section) and ensures that the motor is available where needed to transport cargo. One can imagine that if such a mechanism were not in place the active motor would translocate (without its cargo) toward the plus ends of microtubules and accumulate where they ultimately end; this might lead to their concentration in a region of the cell where they would likely not be needed.

Kinesin-1 is composed of two heavy chains (KHC), which contain the microtubule binding and ATPase activities, and two light chains (KLC; Hackney et al., 1991). While KHC and KLC are encoded by single copy genes in invertebrates, in mammals Kinesin-1 is more complex, with three different KHC genes (KIF5A, KIF5B, and KIF5C, Xia et al., 1998) and three KLC subunits (KLC1, KLC2, and KLC3, Rahman et al., 1998, Junco et al., 2001). Kif5B is ubiquitously expressed; Kif5A and Kif5C are neuronal isoforms (Miki et al., 2001).

Genetic studies of the *kif5A* gene indicate that a mutation in the microtubule binding region of Kif5A is associated with hereditary spastic paraplegia (Blair et al., 2006), Fichera et al., 2004). Hereditary spastic paraplegia is characterized by a severe, progressive degeneration of motor neurons that leads to paralysis of the lower extremeties; thus, this phenotype is consistent with a role for Kif5A in axonal transport. *Kif5A* knockout mice die shortly after birth, but if the gene is linked to a promoter that can be inactivated at later stages of development, losing the function of Kif5A results in a similar phenotype in mice, including hind limb paralysis (Xia et al., 2003).

The other neuronal isoform, Kif5C, seems to play a role in the development of the nervous system. Kif5C is upregulated during development (Kanai et al., 2000, Dathe et al., 2004). *kif5c* knockout mice are viable and appear to have no gross defects in the brain (Kanai et al., 2000). However, as these mice develop, a selective loss of motor neurons, as opposed to sensory neurons, becomes apparent.

kif5b knockout mice die before birth, but embryonic stem cells from Kif5B knockout mice can be cultured to more closely examine the defects associated with the loss of Kif5B (Tanaka et al., 1998). These cultured embryonic stem cells show an abnormal perinuclear clustering of mitochondria. This phenotype is rescued by transfection of either Kif5A or Kif5C, suggesting that these heavy chains can be functionally redundant (Kanai et al., 2000). Knocking out *kif5b* could be embryonic lethal because Kif5A and Kif5C are not expressed in non-neuronal cell types. There is some biochemical evidence that the heavy chains heterodimerize (Kanai et al., 2000), but whether they function separately or together is still unknown.

Domain Structure of Kinesin-1

Kinesin-1 is a heterotetramer, composed of two heavy chains and two light chains (Vale & Fletterick, 1997). The light chains exist in stoichiometric ratios with the heavy chains; that is, little heavy chain can be isolated without the light chain (Hackney et al., 1991). The heavy chains comprise three major domains: the amino terminal motor domain consisting of the catalytic core motor and adjacent neck regions, the central stalk domain, and the carboxy terminal tail and light-chain binding domain (Fig. 1). The light chains are composed of amino

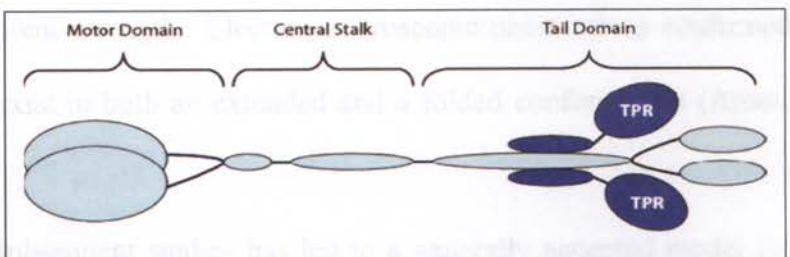

Figure 1: Structure of Kinesin-1. Light blue, heavy chains; Dark blue, light chains.

terminal heptad repeats, which are responsible for the association with the heavy chain, and carboxy terminal TPR domains. The cargo binding domain of Kinesin-1 includes the carboxy termini of the heavy chains along with the TPR domains of the light chains. How the heavy and light chains co-ordinate to bind cargo is not fully understood, but there appear to be distinct cargoes that bind to either the heavy chains or the light chains (Karcher et al., 2002).

Tail Inhibition

Kinesin-1 exists largely as a soluble protein in an inactive conformation (Hollenbeck, 1989, Hackney et al., 1991), and is thought to undergo a conformational change upon cargo binding that activates the motor. The first direct evidence for a major conformational change came from a study by Hackney et al. (1992). Hydrodynamic experiments showed that endogenous Kinesin-1, isolated from bovine brain, transitions from a sedimentation coefficient of 9S to 6S as a function of ionic strength. Electron microscopic observations confirmed that the motor can exist in both an extended and a folded conformation (Amos, 1987).

A series of subsequent studies has led to a generally accepted model for motor inactivation, though the details are still being worked out (Adio et al., 2006). This tail inhibition model proposes that the tails of the heavy chains bind to and inhibit the activity of the head domains. A hinge region in the α-helical stalk region of the heavy chains allows the motor to adopt a folded conformation, and this is stabilized by the light chains. Sucrose density centrifugation and GST

pull-down assays reveal that the heavy chain alone can fold into a compact conformation (Stock et al., 1999). This folding is dependent on three amino acids (IAK) within the last 50 carboxy terminal amino acids and dramatically reduces both the ATPase rate and the microtubule binding affinity of the motor, suggesting that the tail obstructs the head's interaction with microtubules (Hackney & Stock, 2000). Another *in vitro* study, however, showed that, although the tails of the heavy chains reduce ATPase rates, they do not reduce the affinity of the motor for microtubules (Coy et al., 1999). These two studies can be reconciled by the fact that a small region in the heavy chain tail contains a microtubule-binding site (Hackney & Stock, 2000). In one study this portion of the tail was deleted, whereas in the other it was included, which would skew the microtubule binding affinity measurements. In further support of the tail-inhibition model, single molecule motility assays of Cy3-labeled kinesin deletion mutants on immobilized axonemes showed that removal of either the tail or the flexible hinge that allows folding of the protein's stalk resulted in more frequent attachment to and translocation along microtubules (Friedman & Vale, 1999). A study performed *in vivo* suggests that the light chains may contribute to the tail-mediated inactivation of the motor. Immunofluorescence microscopy of COS cells showed that the decoration of microtubules by exogenously expressed heavy chain is eliminated when the light chains are co-expressed, resulting in the soluble distribution of the motor (Verhey et al., 1998) and suggesting that the light chains facilitate the inactivation of the motor by the heavy chains.

Mechanism of Motility

Kinesin-1 is a highly processive motor, which means that it can travel hundreds of steps each time it encounters a microtubule (Hackney, 1995, Vale et al., 1996). This processive motion requires two heads (Hancock & Howard, 1998) and implies that the two heads must co-ordinate their activities, because to travel that many steps without dissociating requires that one of the two heads remain attached to the microtubule (Adio et al., 2006). A large body of work has contributed to the development of a 'hand-over-hand' model for Kinesin-1 translocation that explains this processive motion.

The general features of this model are that while one head anchors the motor to the microtubule, the other head swings forward and attaches in front of the rear head (Fig. 2). While both heads are attached the forward head undergoes an ATP-dependent conformational change in the neck linker region. This conformational change is accompanied by the release of the rear head from the microtubule, which then swings forward, at which point the cycle is repeated (Vale & Milligan, 2000).

Figure 2: Kinesin-1 walks hand-over-hand. This cartoon starts as the rear head has just swung forward. After it attaches, Kinesin-1 exists in an intermediate state when two heads are attached. The rear head hydrolyzes ATP resulting in a conformational change that allows the rear head to swing forward. **From www.ucsf.valelab.edu**

The stepping behavior of Kinesin-1 was first observed using a microscopic technique called the optical trap. In this method, a very small, but very bright

spot of light is used to place a bead with an attached motor near immobilized microtubules. The motor will bind and move along the microtubule, with the bead as its cargo. Tension applied to the trap reduces the Brownian motion of the bead to the nanometer level so that the stepping motion of the bead now represents the movement of the motor (Asbury, 2005). Using this method, Svoboda et al (1993) analyzed the motion of Kinesin-1-coated beads and found that they moved, on average, in 8-nm increments. The individual motor domains of single Kinesin-1 dimers have also recently been directly observed using FIONA (Fluorescence Imaging One-Nanometer Accuracy), a high-resolution microscopy technique that allows the tracking of a single Cy3 dye molecule with nanometer accuracy (Yildiz et al., 2003). One head of a truncated dimer of Kinesin-1 was tagged with a Cy3 fluorophore and the dye's position was monitored as the motor moved on microtubules that were immobilized on a coverslip (Yildiz et al., 2004). The data showed that the dye moves in ~16-nm increments, which is consistent with each head taking one 8-nm step. This stepping distance is consistent with Kinesin-1 binding to the β-subunit of microtubules (Song & Mandelkow, 1993, Harrison et al., 1993), which are 8-nm apart in a microtubule protofilament. With each 8-nm step, Kinesin-1 hydrolyzes one ATP, indicating that the enzymatic cycle is tightly coupled to the mechanochemical cycle of the motor (Schnitzer & Block, 1997, Hua et al., 1997, Coy et al., 1999).

Kinesin-3

The first member of this family was identified when Hall & Hedgecock examined the ultrastructural defects of *C. elegans* mutants that had been screened for an 'uncoordinated' phenotype. *Unc104* mutants contained few vesicles in their axon terminals and made only a small number of synapses (Hall & Hedgecock, 1991). In contrast, the neuronal cell bodies contained a surplus of similar vesicles tethered together in the cytoplasm. Based on these phenotypical observations, Hall & Hedgecock hypothesized that *unc104* mutants are defective in the antergorade axonal transport of synaptic vesicles. DNA sequence analysis of *unc104* revealed the presence of what are now known as the defining sequences of kinesin motor proteins, the ATPase and microtubule binding domains of the catalytic motor head (Otsuka et al., 1991). The mammalian homolog of Unc104 was later identified through a PCR-based screen for kinesin motor-like domains in mouse brain and named Kif1A (Aizawa et al., 1992).

Numerous studies point toward a role of Unc104/Kif1A in the transport of synaptic vesicles. Immunoisolation of axonal vesicles from mouse nervous tissue showed that Kif1A associates with a particular subset of vesicles that contained synaptophysin, synaptotagmin and Rab3A, but did not contain other proteins such as syntaxin-1, SNAP25 and SV2 (Okada et al., 1995). Other known kinesins, such as Kinesin-1 and Kinesin-2 are not detectable on these organelles by Western Blot. One way to test the axonal transport of a cargo is to ligate the sciatic nerve of living mice. Cargoes that are anterogradely transported, including synaptic vesicle proteins, will accumulate on the proximal side of the ligation. Using this method, the accumulation of specific proteins was investigated in *kif1A*

knockout mice. Consistent with the biochemical studies, syntaxin-1A, but not synaptotagmin, accumulates at the proximal side of the nerve ligation, suggesting that syntaxin-1A is not transported by Kif1A, whereas synaptotagmin is (Yonekawa et al., 1998). However, immunohistochemical analysis showed less intense and less dense staining in synaptic areas of spinal cord sections of both the Kif1A-associated synaptic vesicle protein synaptophysin, and the non-Kif1A-associated protein SV2. This finding suggests that either Kif1A transports more than one subset of vesicles, or that the knockdown of Kif1A has effects on other kinesin motor proteins.

There is evidence to suggest that Unc104's association with its cargo depends on interactions with lipids rather than proteins. Unc104/Kif1A contains a pleckstrin homology (PH) domain at its tail that is thought to interact with specific lipids in membranes (Klopfenstein et al., 2002). In rescue experiments performed in an *unc104* null background, transfection of an Unc104 motor lacking the PH domain could not rescue the uncoordinated phenotype (Klopfenstein et al., 2004). Furthermore, point mutations that abolish the interaction of the PH domain with its preferred lipid, PtdIns(4,5)P2, reduced the velocity and processivity of Unc104-GFP in *C. elegans* neurons. These results suggest that Unc104 binds to the membrane of vesicles via its PH domain. Whether such a mechanism is sufficient to account for the specificity of Unc104 cargo binding is still an open question, but it may be that certain types of vesicles contain more PtdIns(4,5)P2 than others, and therefore would have a higher likelihood of binding to Unc104.

Mechanism of Motility

The motility mechanism of Kif1A has been controversial. One model posits that Kif1A translocates as a monomer, a process referred to as "biased diffusion", whereas an alternative model holds that Kif1A translocates as a dimer, taking successive steps much like Kif5. Though I review the arguments in support of both models, I believe that the preponderance of the evidence favors the second model.

Like Kif5, Kif1A contains an amino terminal ~330 amino acid catalytic motor domain which is connected to the neck coil via a linker region (Schnapp, 2003). Following the neck coil is a forkhead-associated (FHA) domain, which plays a role in regulating the activity of the motor (Lee et al, 2004). Cargo binds to the COOH terminal tail region, which contains the PH domain. Unlike Kif5, however, Kif1A exists primarily as a monomer (Okada et al, 1995, Pierce et al, 1999). In addition, Kif1A is unique among kinesins in that it contains an insertion of several lysine residues (k-loop) in the region adjacent to the minimal catalytic head domain (Okada et al., 1995).

These two properties were the basis of a series of studies that led to the model of monomeric, or single-headed, processivity. Monomeric Kif1A binds to microtubules *in vitro*, and accumulates at the plus ends of microtubules, suggesting that the monomer moves directionally along microtubules (Okada et al., 1999). In contrast, Kif5 monomers fail to accumulate at the ends of microtubules. The crystal structure of Kif1A reveals that the k-loop in the neck

linker region is ideally positioned to interact with the microtubule when the motor is docked (Kikkawa et al., 2000). Furthermore, k-loop mutants lacking some or all of the lysine residues are less processive in single molecule motility assays, and this behavior can be mimicked by removal of the C-terminal tail of tubulin by subtilisin digestion (Okada et al., 2000). These results led Okada et al. (2000) to propose the "biased diffusion" model for Kif1A translocation. In this model the positively charged lysine residues of the Kif1A motor domain's k-loop facilitate the attachment of the motor to the negatively charged C-terminal of tubulin, which prevents the motor from diffusing away from the microtubule while the monomeric head detaches and steps forward.

In the studies described above, the observed velocities of Kif1A are about ten-fold slower (0.14μm/s) than those observed for the full-length motor in living cells (Zhou et al., 2001, Lee et al., 2003) and *in vitro* (Okada et al., 1995). In addition, biased diffusion was not observed in another *in vitro* study using both the monomeric and dimeric *C. elegans* motor domain (Pierce et al., 1999), though the authors later stated that they could induce the phenomenon by adding extra positively charged residues to the neck linker region and conducting the assay under specific buffer conditions (Tomishige et al., 2002). Thus, the single-headed model of processivity does not fully explain the translocation properties of Kif1A.

Clarification on the mechanism of Kif1A motility has come from studies by Klopfenstein et al. (2002) who investigated the Unc104-mediated movement of liposomes. They found that liposome movement by monomeric Unc104 motors showed a very steep dependence on PtdIns(4,5)P2 concentration, even

though liposome binding was non-cooperative (Klopfenstein et al., 2002). The monomeric motor moves particles under conditions which concentrate the PH domain of the motor's cargo binding tail on the lipid bilayers, suggesting that clustering of Unc104 in PtdIns(4,5)P2-containing rafts may activate the motor. A mutation predicted to destabilize the neck coil inhibits liposome movement (Klopfenstein et al., 2002). These results suggest that binding to liposome cargoes induces dimerization of the motor, which enables processive translocation. This hypothesis was confirmed by single molecule *in vitro* studies of chimeric motor proteins. A truncated Kif1A motor that is artificially dimerized with either a leucine zipper or the coiled coil domain of Kif5 moves processively along microtubules (Tomishige et al., 2002).

These studies suggest that Kif1A functions as a dimer. Yet, it exists mainly as a monomer. These two facts can be reconciled by considering that the monomeric state of Kif1A serves as its inactivation mechanism, much like the folded conformation of Kif5 inactivates that motor. In support of this hypothesis cryo-electron microscopy revealed two states of Unc104 bound to microtubules: a monomeric state in which two neck helices form an intramolecular, parallel coiled coil, and a dimeric state in which the neck helices form an intermolecular coiled coil (Al-Bassam et al., 2003). Deletion of the flexible hinge separating the neck helices abolishes the intramolecular folded conformation, indicating that it acts as a spacer to accommodate the parallel coiled-coil configuration. The neck hinge deletion does not alter motor velocity *in vitro* but produces a severe uncoordinated phenotype in transgenic *C. elegans*. This phenotype is characteristic of *unc104*

mutants, suggesting that the folded conformation plays an important role in motor regulation. A similar mechanism of activation was proposed by Lee et al. (2004), though the domains involved differ slightly. Using an *in vivo* functional assay, they showed that the FHA domain of Kif1A negatively regulates the activity of the motor. They found that disrupting the interaction between the FHA domain and the second coil domain results in a dimerized motor that is constitutively active, both *in vitro* and *in vivo*. This result raises the interesting possibility that the FHA – second coiled coil interaction negatively regulates the motor's activity by keeping Kif1A in the monomeric state, which is consistent with the finding by Al-Bassam et al. (2003) that the neck hinge and FHA domain deletions do not rescue the *unc104* null phenotype.

In sum, these studies strongly argue for a model of the regulation of Kif1A motility that involves a switch between a self-folded, inactive state and a dimerized, active state that is dependent on the FHA domain. Cargo binding may be the switch that regulates the transition from the inactive, monomeric state to the active dimerized state *in vivo*.

The Selectivity of Kinesin-driven Transport in Neurons

As described in Chapter 1, proteins synthesized in the neuronal cell body are transported via kinesin-mediated transport to their ultimate destinations. How motors contribute to the organization of this transport is still largely unknown, although clues are emerging. There is evidence to suggest that preferential transport plays an important role in localizing proteins in neurons. Preferential

transport in this context refers to the transport of a protein via the preferential translocation of kinesin motor proteins along distinct microtubule populations that lead to different subcellular destinations. For example, a protein that is localized to dendritic spines would associate with a motor that recognizes dendritic microtubules and preferentially translocates along those microtubules. In this way, the protein's localization could depend, at least in part, on the motor's ability to choose a particular route.

Dendritic Cargo

Signals in the cytosolic domain of dendritic proteins govern their sorting into carriers at the *trans*-golgi network (TGN) that are transported throughout the somatodendritic domain, but do not enter the axon. When these sorting signals are mutated, dendritic proteins are transported into both dendrites and the axon and are no longer polarized to the dendritic cell surface (Jareb & Banker, 1998, West et al., 1997). It was once hypothesized that carriers containing dendritic proteins are excluded from the axon based solely on the directionality of their motors (Black & Baas, 1989). In mature hippocampal neurons, dendrites contain both minus and plus end-out microtubules, whereas axons contain only plus-end out microtubules. Thus, if dendritic carriers were exclusively transported by a minus-end-directed motor they would be excluded from the axon merely by virtue of the directionality of the transporting motor. However, dendritic carriers are transported into dendrites and excluded from the axon very early in development (Silverman et al., 2001), before the presence of minus end-out microtubules in

dendrites (Black & Baas, 1989), indicating that these carriers are transported by a plus end-directed kinesin. This indicates that the motors transporting dendritic cargoes distinguish more than the directionality of microtubules, and suggests that there may be a "dendritic" motor that recognizes biochemical modifications on microtubules that lead to dendrites but not the axon.

Axonal Cargo

The role of selective transport for axonal proteins is more difficult to decipher. One would not expect axonal proteins to be completely excluded from the cell body and dendrites, because they are synthesized in that domain. Though carriers containing the axonal protein NgCAM-GFP are indeed transported throughout both domains of the cell, they appear to be preferentially transported into the axon by a factor of 2-5-fold (Burack et al., 2000, Nakata & Hirokawa, 2003). A study examining the transport of the axonal cargo amyloid precursor protein (APP) provides further data that preferential transport plays a role in axonal targeting. Simons et al (1995) found that APP is first directly targeted to the axon, then transcytoses to the dendritic domain. The only clear evidence for the *exclusion* of axonal carriers from dendrites is provided by Kanaani et al. (2004). They investigated the targeting of the GABA-synthesizing enzyme GAD65 in hippocampal neurons, and found that it is transported directly into the axon in axonal EEA1-negative, rab5-positive endosomes. Though mechanisms downstream of transport are known to be important in the polarization of some

axonal cargo (Sampo et al, 2003), the data discussed above indicates that their preferential transport may also contribute to their localization.

Evidence for a Selective Motor

The above studies examined the transport of *cargoes*, which are moved by associating with the motors that transport them along microtubules. The transport pathways of these cargoes may be an indication of the selective translocation of the underlying motor along a subset of microtubules, but the assay is indirect. A study by Nakata & Hirokawa (2003) was the first to look directly at the translocation of a motor in the absence of cargo. As a measure of where the motor translocates in the neuron, they assessed the accumulation of a constitutively active, fluorescently tagged version in mature hippocampal neurons. They found that the Kinesin-1 family member Kif5B accumulates selectively in the axon, leading the authors to suggest that this kinesin translocates preferentially along axonal microtubules. However, their study was performed on mature hippocampal neurons; at this stage of development a comparison of the localization of a constitutively active plus end-directed kinesin is complicated by differences in microtubule polarity orientations in axons and dendrites. While axons contain only plus end out microtubules, dendrites contain microtubules of mixed polarity. Thus, there are two possible explanations for why Kif5B fails to accumulate in mature dendrites. Either it translocates bi-directionally, never accumulating at the tips merely by virtue of the organization of microtubules in that domain, or it distinguishes between microtubules in the axon and those in the

dendrites, and preferentially translocates along those in the axon. The third chapter of this dissertation distinguishes between these two possibilities.

The Microtubule Cytoskeleton

Any discussion of kinesins must consider the microtubule cytoskeleton along which all kinesins travel. Microtubules are composed of parallel protofilaments, which are linear polymers of αβ tubulin dimers (Nogales et al., 2000). The αβ tubulin dimers add longitudinally to the protofilaments so that the β-subunit is exposed at one end, referred to as the minus end, and the α-subunit is exposed at the other, "plus", end. Thus, microtubules exhibit an intrinsic polarity. The plus ends of microtubules are highly dynamic and switch stochastically between growing and shrinking phases, a non-equilibrium behavior termed dynamic instability (Desai & Mitchison, 1997). The same basic building blocks, α and β tubulin, are responsible for the function of microtubules in a diverse array of important cellular processes, such as mitotic spindle segregation, flagellar and cilial motility, and intracellular organelle transport.

Microtubule diversity is generated by a host of reversible post-translational modifications (PTMs) of tubulin as well as by association with various microtubule-associated proteins (MAPs), which can also be modified post-translationally. Both α- and β-tubulin undergo post-translational modifications, including detyrosination, acetylation, phosphorylation, polyglutamylation, and polyglycylation (Rosenbaum, 2000). Most modifications occur on the carboxy terminal domains of the tubulin subunits, which are located

on the outside of the microtubule, where they are well-positioned to influence interactions with other proteins, including motors (Nogales et al., 1998). Microtubule binding proteins include those that bind along the length of the microtubule, such as MAP2, MAP1A, MAP1B and tau, as well as plus end tip-binding proteins, such as EB1 and CLIP170.

Evidence for Different Populations of Microtubules

As discussed in the introduction, this dissertation provides data that the molecular motor Kif5C selectively translocates along a subpopulation of microtubules in neurons, implying that there are distinct populations of microtubules within the cell. While the specific microtubule modifications responsible for the differential interaction of the motor with microtubules remains unknown, there is evidence in the literature that these molecularly distinct microtubules exist in the same cell, sometimes within close proximity to each other. Double immunofluorescence studies in cultured kidney cells show that detyrosinated and tyrosinated microtubules do not overlap, but instead comprise distinct subsets of the total population of microtubules (Gundersen et al., 1984). In another approach, Miller et al. (1987) used a cold block to accumulate moving vesicles in lobster axons and found by electron microscopy that the vesicles accumulate along some microtubules, but not neighboring microtubules. Immunogold labeling of axonemes from the flagella of the green alga *Chlamydomonas reinhardtii* revealed that Klp1, a member of the Kinesin-9

family, is restricted to one of the two central pair microtubules (Bernstein et al., 1994).

Another approach that distinguishes distinctly modified subpopulations of microtubules involves the use of biochemical methods. Polyglutamylation levels of tubulin can differentially regulate the association of MAPs with microtubules. *In vitro* binding studies show that the relative affinity of tau, MAP2 and MAP1B is low for unmodified tubulin, progressively increases as a few polyglutamyl chains are added, and then decreases as the polyglutamyl side chain length increases (Boucher et al., 1994, Bonnet et al., 2001). Polyglutamylation levels have different effects on different MAPs. MAP1A has the selective property of maintaining high affinity for highly glutamylated tubulin, whereas binding of another MAP, STOP, is not dependent on polyglutamylation levels (Bonnet et al., 2002). This differential regulation exerted by polyglutamylation toward different MAPs might facilitate their selective recruitment into distinct microtubule populations, hence modulating the functional properties of microtubules.

Microtubule Modifications That Affect Kif5

The only post-translational modification known to directly affect the interaction of Kinesin-1 with microtubules is polyglutamylation. *In vitro* binding studies show that the Kinesin-1 motor domain exhibits optimal binding to tubulin modified by ~3 glutamyl residues; binding affinity decreases with increased polygutamyl chain length (Larcher et al., 1996). An indirect measure of how post-translational modifications affect kinesins can be obtained by assessing

microtubule-based transport of cargo. Microinjection of an anti-polyglutamylation antibody into cultured melanophores interferes with kinesin-dependent pigment granule dispersion, but not dynein-dependent aggregation (Klotz et al., 1999). The lack of effect on dynein-mediated transport indicates that this modification could be a specific regulator of kinesin-mediated transport. In a genetic approach, mutations of tubulin glycylation sites in *Tetrahymena* result in defects in intraflagellar transport (Redeker et al., 2005). Though Kinesin-1 itself is not thought to mediate melanophore or intraflagellar transport, these studies support the model that post-translational modifications to microtubules can regulate kinesin-based transport.

MAPs also regulate the interaction of kinesins with microtubules. Using an *in vitro* assay, Seitz et al. (2002) used total internal reflection (TIRF) microscopy to analyze the effect of different MAPs on the translocation of single truncated Kinesin-1 motors. They found that the longest human tau isoform, htau40, decreases the frequency of attachment to microtubules, but has no effects on the motor's velocity or run length. Truncated Kinesin-1 exhibits less affinity for microtubules that are decorated with htau40, and hydrolyzes less ATP in the presence of htau40-decorated microtubules. Taken together, these results suggest that tau interferes with the attachment of Kinesin-1 to the microtubule, but not its translocation once the motor has attached. Interestingly, this study found that different MAPs reduced Kinesin-1's affinity for microtubules to different degrees. MAP2c is the most effective at inhibiting attachment, which is consistent with MAP2c's high affinity for microtubules. However, a MAP's affinity for

microtubules does not always correlate with its ability to inhibit kinesin attachment. For example, the long isoform of human tau, htau40, binds more tightly to microtubules than the juvenile isoform, htau23, but does not inhibit attachment as well. These findings indicate that different MAPs affect the behavior of Kinesin-1 differently, and thus the differential distribution of MAPs could govern for the efficiency of Kinesin-1 translocation along a distinct population of microtubules.

The effects of MAPs on vesicle transport have also been investigated and serve as an indirect measure of their influence on kinesin motor proteins. Overexpression of tau leads to impaired localization of mitochondria in CHO cells and in differentiated N2a cells, suggesting that tau interferes with their transport (Ebneth et al., 1998). Direct observation of vesicles containing VSVG-GFP showed that tau transfection reduces the number of plus end-directed movements (Trinczek et al., 1999). Interestingly, tau expression also reduces the run length of VSVG-containing vesicles, which is in contrast to *in vitro* observations on individual motors in the presence of tau (Seitz et al., 2002). There are two plausible explanations for the discrepancy. First, the *in vitro* assay required low ionic strength, and since both kinesin and MAP interactions with microtubules depend on salt concentration (Vale & Fletterick, 1997), it is conceivable that MAPs interact more efficiently with microtubules at the higher salt concentration found *in vivo* and thus present more effective obstacles in that environment. Second, multiple motors could be responsible for the transport of one vesicle. If this were the case, a reduced attachment rate of individual motors

might manifest itself as a reduced run length of the vesicle. Thus, these studies indicate that both post-translational modifications and MAPs can regulate kinesin-dependent transport.

Dynamic Instability

Dynamic instability refers to the microtubule's ability to rapidly and stochastically switch between period of growth and periods of shrinkage. This behavior is crucial to the function of microtubules during cellular processes that require the rapid rearrangement of the cytoskeleton, such as cell migration, growth and mitosis. I discuss the dynamic behavior of microtubules here because Chapter 4 tests the hypothesis that differences in microtubule dynamics contribute to the selective translocation of Kif5.

The four parameters that characterize dynamic stability are rate of growth, rate of shrinking, frequency of transition from growth to shrinkage (catastrophe) and from shrinkage to growth (rescue). Growth and shrinkage occur at the microtubule ends through the addition or removal of tubulin dimers.

Dynamic instability is regulated by two classes of proteins: Structural MAPs and plus end binding proteins. Structural MAPs, such as tau and MAP2 bind along the length of the microtubules and are thought to stabilize them. Purified bovine brain MAPs microinjected into cultured cells containing rhodamine-labeled tubulin greatly reduces dynamic instability (Dhamodharan & Wadsworth, 1995). *In vitro* studies using labeled MAP2 showed that microtubule depolymerization stops in areas where this MAP is highly concentrated on the

microtubule (Ichihara et al., 2001). Photobleaching of MAP2-decorated microtubules revealed distinct regions along the microtubule that bleach at a slower rate; these regions are correlated with increased rescue frequency and stops in depolymerization. Further evidence that MAPs stabilize microtubules is supported by studies on the effects of the microtubule-severing protein, katanin, on MAP-decorated microtubules. The frog homolog of MAP4 reduces the microtubule-severing activity of katanin *in vitro* (McNally et al., 2004). Tau appears to act in a similar fashion in living neurons. Microtubules in the axon are normally more resistant to katanin (Baas & Qiang, 2005). siRNA depletion of tau in hippocampal neurons results in a loss of protection from katanin (Qiang et al., 2006). Protection from severing by katanin is not a general property of MAP-stabilized microtubules, however, as MAP1B does not prevent katanin-induced severing; nor does the microtubule-stabilizing drug taxol (Qiang et al., 2006).

Plus end-binding proteins comprise the second class of proteins known to regulate dynamic instability. The two best known proteins in this class are EB1 and CLIP170, both of which bind to the plus ends of actively polymerizing microtubules and are thought to promote polymerization. Immunodepletion of EB1 from *Xenopus* egg extracts reduces microtubule length, and this is rescued by readdition of EB1 (Tirnauer et al., 2002). In Drosophila S2 cells, siRNA knockdown of endogenous EB1 reduces the number of elongating microtubules (Rogers et al., 2002). EB1 appears to have similar effects *in vitro*; addition of EB1 to nucleated microtubules results in significantly longer microtubules (Ligon et al., 2003). Expression of a dominant negative CLIP170 construct that abolishes

its interaction with microtubule plus ends results in a decrease in the frequency of microtubule rescue events, suggesting that this plus end binding protein plays an important role in the switch from the paused or depolymerizing state to the polymerizing state (Komarova et al., 2002). These results suggest that both EB1 and CLIP170 promote the polymerization of microtubules. How they act in concert with each other and with other plus end binding proteins is still an active area of research (Vaughan, 2004, 2005).

The Development of Neuronal Polarity

Morphological Changes in Culture

Hippocampal neurons follow a stereotypic pattern of development in culture, which was first described by Dotti et al. (1988). Several hours after plating, neurons extend 3-5 similar processes (stage 2, Fig. 3). Though the morphology of these processes can vary slightly, they are considered to be

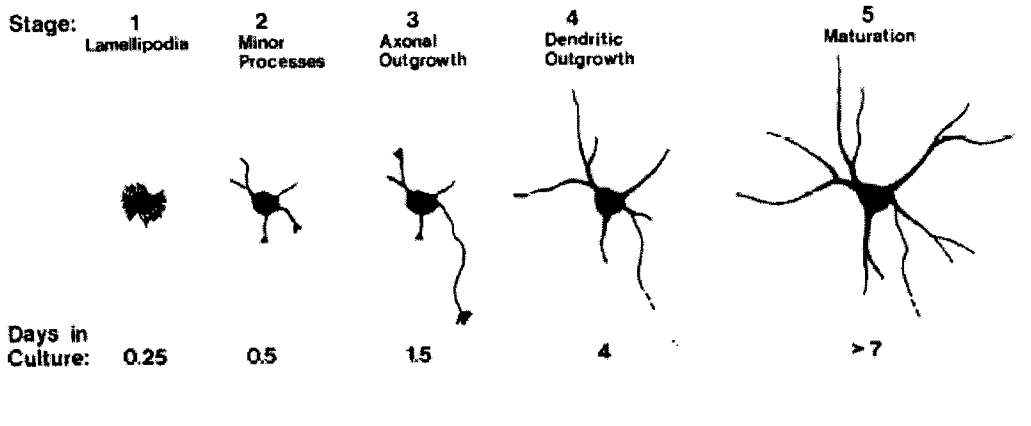

Figure 3: Morphological Changes in Culture. After plating, neurons initially extend several neurites (stage 2). After ~24h, one neurite undergoes a prolonged growth spurt that specifies it as the axon. Over the next 4 days, the dendrites begin to elongate and acquire their characteristic tapered shape. **From Craig & Banker, 1994**

functionally equivalent. Within the next 24-30 hours, one of these processes undergoes a prolonged growth spurt, becoming the axon (stage 3). Over the next ~4 days the dendrites begin to develop and gradually acquire their characteristic tapered morphology (stage 4).

The microtubule organization is different in stage 3 neurons than in mature neurons (Baas et al., 1989). In stage 3 neurons, microtubules are oriented the same way in all neurites. Their plus-ends point away from the cell body, toward the tips of processes, and their minus-ends point toward the cell body. As the neuron matures (stage 4), differences in microtubule orientation in the two domains arise. Microtubules in the axon remain uniformly oriented, with their plus-ends pointing toward the growth cone. In contrast, microtubules in mature dendrites have a mixture of orientations. That is, some microtubules have their plus end directed away from the cell body, while others have their plus-end directed toward the cell body. This differential organization of microtubules has implications for kinesin-mediated transport, because kinesins are unidirectional. A plus-end directed kinesin, for example, can translocate anterogradely, but not retrogradely, in the axon and immature dendrites of a stage 3 neuron. The same is true in mature axons. But in mature dendrites, plus-end-directed kinesins can travel bi-directionally.

Axon Specification

How does only one of many seemingly identical neurites differentiate to become the axon? *In vivo*, this process likely involves extracellular cues that reach a single neurite and subsequently trigger internal signaling cascades within the growth cone of just that neurite (Horton & Ehlers, 2003). The downstream effectors of these signals rearrange the actin and microtubule cytoskeleton to produce growth (Fig. 4). In culture, exposing one neurite to an appropriate extracellular cue, such as an adhesion molecule, can trigger axon specification (Esch et al., 1999, Menager et al., 2004). However, neurons in culture develop polarity in the absence of spatially organized extracellular cues, indicating that they have an intrinsic program that leads to the specification of one neurite as the axon.

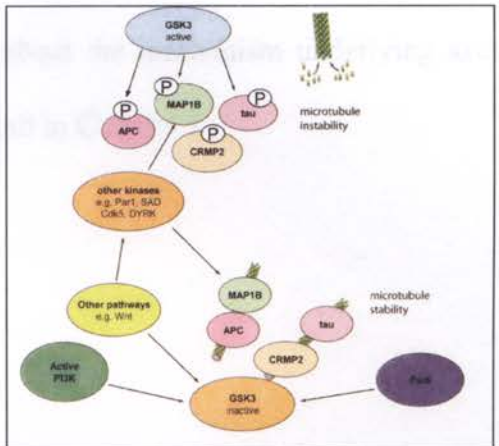

Figure 4: Signaling Proteins In Axon Specification. **Adapted from Wiggin et al. (2005)**

The prevailing model of axon specification in culture holds that each neurite at stage 2 is equally capable of becoming the axon (Goslin & Banker, 1989, Shi et al., 2003). Stochastic enrichments of axon-inducing signaling proteins in a single growth cone are augmented by a positive feedback loop; once a certain threshold is reached, a signaling cascade is triggered and results in the prolonged growth spurt that specifies that neurite as the axon.

A number of studies on hippocampal neurons in culture have identified signaling molecules that contribute to axon specification (Fig. 4; reviewed in Wiggin et al., 2005). These proteins were often first identified as important in axon specification by their selective localization to the axonal growth cone at stage 3. The restricted localization or activation of these proteins in one neurite at stage 2 was thought to precede the nascent axon's outgrowth. However, these studies relied on fixed images at the two stages of development – unpolarized stage 2 neurons and polarized stage 3 neurons. The findings presented in this dissertation indicate that the selective localization of an axonal protein at stage 2 to a single neurite does not necessarily predict that neurite will become the axon. These findings raise important questions about the mechanism underlying axon specification and are discussed in more detail in Chapter 5.

Chapter 3

A Change in the Selective Translocation of the Kinesin-1 Motor Domain Marks the Initial Specification of the Axon

Catherine Selph[1], Bruce Schnapp[2] and Gary A. Banker[1]

[1]Center for Research on Occupational and Environmental Toxicology and [2]Department of Cell and Developmental Biology, Oregon Health & Science University, Portland, OR 97239

Abstract

We used the accumulation of constitutively active kinesin motor domains as a measure of where kinesins translocate in developing neurons. Throughout development, truncated Kinesin-3 accumulates at the tips of all neurites. In contrast, Kinesin-1 accumulates *selectively* in only a subset of neurites. Before neurons become polarized, truncated Kinesin-1 transiently accumulates in one neurite at a time. Coincident with axon specification, truncated Kinesin-1 accumulates only in the emerging axon and no longer appears in any other neurite. The translocation of Kinesin-1 along a biochemically distinct track leading to the nascent axon could ensure the selective delivery of Kinesin-1 cargoes to the axon and hence contribute to its molecular specification. Imaging YFP-tagged truncated Kinesin-1 provides the most precise definition to date of when neuronal polarity first emerges and allows visualization of the molecular differentiation of the axon in real time.

Introduction

To maintain the functional differences between axons and dendrites, neurons must traffic distinct sets of proteins to each compartment selectively, a process that involves microtubule-based transport (Craig and Banker, 1994; Horton and Ehlers, 2003). Dendritically polarized proteins are transported into dendrites but excluded from the axon while other proteins are preferentially transported into the axon (Burack et al., 2000; Nakata and Hirokawa, 2003). Whether selective microtubule-based transport also has a role in the initial specification of axons and dendrites is still unknown (Bradke and Dotti, 1997; Nishimura et al., 2004). This possibility is appealing because axon specification is thought to involve the selective localization of signaling proteins within a single neurite and this likely depends on microtubule-based transport (Wiggin et al., 2005). To address this possibility, we asked whether selective kinesin-driven transport occurs in immature neurons *undergoing* axon specification. As a measure of kinesin-driven transport we examined the localization of constitutively active, YFP-tagged kinesins. We focused on the Kinesin-1 family member Kif5 because a previous study (Nakata and Hirokawa, 2003) indicated that its motor domain accumulates in axons but not in dendrites. Specifically, we asked whether the selective accumulation of the Kif5 motor domain in a single growth cone arises early enough in development for selective transport to play a mechanistic role in axon specification.

Hippocampal neurons in culture initially put out several short, apparently identical neurites (developmental stage 2, Dotti et al., 1988). Polarity

first emerges when one neurite undergoes an extended period of growth and becomes the axon (stage 3). The remaining neurites subsequently become dendrites (stage 4). Some of the signaling pathways important in axon specification are becoming clear (Wiggin et al., 2005), but how these signaling proteins are localized to and activated in a single neurite is still not known. Selective transport would be one way to ensure that axon-inducing signaling proteins become restricted to a single neurite.

There are two general mechanisms that can explain the selectivity of kinesin-driven transport. One possibility is that cargoes regulate motor activity differentially. In this model, binding of axonal cargoes causes a kinesin to translocate more efficiently on microtubules leading into the axon, whereas binding dendritic cargo directs this kinesin to the dendrites. For example, the distribution of Kif5 in cultured hippocampal neurons may be altered by overexpression of GRIP-1, a dendritically localized protein (Setou et al., 2002), or JIP-1, a Kif5 cargo that is present in axons (Verhey et al., 2001). On the other hand, the Kif5 motor domain may translocate preferentially on axonal microtubules, independent of cargo binding. In support of this model, a constitutively active version of Kif5 that lacks the cargo-binding tail domain selectively accumulates at the ends of axons, but not dendrites, in mature (stage 4) neurons (Nakata and Hirokawa, 2003).

The mechanism by which truncated Kif5 selectively accumulates in the axons of mature neurons is unclear because mature axons and dendrites differ in the polarity orientation of their microtubules (Baas et al., 1989). In axons, more

than 90% of the microtubules are oriented with their plus ends directed away from the cell body, while dendrites contain an equal number of microtubules oriented with plus ends directed away from or toward the cell body. Thus, a constitutively active plus-end directed motor such as truncated Kif5 could translocate bi-directionally in dendrites, but only in the anterograde direction once it enters the axon. This alone might explain why truncated Kif5 selectively accumulates in the axon. An alternate possibility is that truncated Kif5 translocates preferentially into the axon because it recognizes biochemical differences between axonal and dendritic microtubules.

Here, we distinguished between these two possible mechanisms by examining the transport of truncated Kif5 at stage 3 of development, when the microtubule polarity orientation in dendrites and axons is identical (> 90% with plus ends out in both; Baas et al., 1989; Stepanova et al., 2003). We found that, in spite of the similar organization of microtubules in axons and dendrites at this stage, truncated Kif5 selectively accumulated in axon tips. A similar construct containing the motor domain of the Kinesin-3 family member Kif1A was not selective, and instead accumulated in the tips of both axons and dendrites. These results favor a model in which biochemical differences between axons and dendrites regulate the translocation efficiency of truncated Kif5, but not that of Kif1A. Live-cell imaging of neurons at stage 2 of development, prior to axon specification, showed that truncated Kif5 underwent stochastic cycles of accumulation in and disappearance from the growth cones of different neurites. Coincident with the growth of the emerging axon, truncated Kif5 stably

accumulated only in that growth cone and no longer appeared in any other neurite. These findings raise the possibility that the selective transport of Kif5 cargoes along a molecularly distinct pathway contributes to specification of the axon.

Results

Truncated Kinesin-1 preferentially translocates along microtubules in axons.

We used the accumulation of Kinesin-1 and Kinesin-3 motor domains as a measure of where these motors undergo translocation in neurons. Because these truncated motors are *not* auto-inhibited like the wild-type motors, whenever they encounter a microtubule and bind to it, they move processively toward its plus end, as documented by *in vitro*, single molecule imaging (Friedman and Vale, 1999; Tomishige et al., 2002). In neurites whose microtubules are uniformly oriented plus end-out, active transport continuously drives these motors distally. In support of this interpretation, kinesin mutants that are unable to translocate processively along microtubules do not accumulate at neurite tips (Supp. Fig. 1; see also Nakata and Hirokawa, 2003; Lee et al., 2004).

We first focused on the question of whether the accumulation of the Kif5 motor domain in axons, but not dendrites, of mature neurons (Nakata and Hirokawa, 2003) is due to differences in microtubule polarity orientation or to differences in the motor's translocation efficiency in the two domains. We examined the localization of Kif5C^{560}-YFP (a truncated version of Kif5C

consisting of the motor, neck linker, neck coil and first stalk regions; Fig. 1A) at developmental stage 3, before the appearance of minus end-out microtubules in dendrites. Kif5C^{560}-YFP brightly labeled the tips of nearly every axon, but almost never labeled dendritic growth cones (Fig. 1B). In fact, Kif5C^{560}-YFP was barely detectable in cell bodies, where it is synthesized, or along axon shafts, even though it must pass through these regions en route to the axon tip, indicating that Kif5C^{560} translocates efficiently when expressed in cells. For comparison, we determined the localization of a truncated Kif1A (Kif1A^{396}; Fig. 1A). In contrast to Kif5C^{560}, Kif1A^{396} labeled dendritic as well as axonal growth cones (Fig. 1B). To confirm that the axonal localization of Kif5C^{560} was due to its motor domain, we compared its localization to that of a chimera (Kif1A^{cc}) consisting of the motor and neck linker domains of Kif1A and the neck coil and dimerization domains of Kif5C (Fig. 1A). This construct also accumulated in both axons and dendrites. Quantitative analysis confirmed this difference in localization between Kif5C^{560} and Kif1A^{cc}; 66% of the growth cones of immature dendrites showed a pronounced accumulation of Kif1A^{cc}, while Kif5C^{560} accumulated in only 3% (T-test, $p<0.001$). Both motors labeled almost every axonal growth cone (KIF1A^{cc}, 96%; Kif5C^{560}, 92%). At this stage of development, immature dendrites are still relatively short and undergo cycles of growth and retraction. Time-lapse imaging of a stage 3 neuron revealed that accumulated Kif1A^{396} could be lost from a retracting neurite (Supp. Movie 1). This probably explains why Kif1A^{396} did not accumulate in every minor neurite. These findings indicate that the selective accumulation of Kif5C^{560} in axonal growth cones is due not to differences in

microtubule polarity orientation, but rather reflects its more efficient translocation in the axon. Kif5C^{560} selectivity is a property of the motor and neck linker regions of Kif5C.

Before axon specification, truncated Kinesin-1 selectively and transiently accumulates in different neurites.

To determine whether the selective translocation of Kif5C^{560} arises before axon specification, we used live cell imaging to examine the dynamics of its accumulation during stage 2 of development. As a control, we first investigated the dynamics of Kif1A^{cc} at this stage. As expected from observations in stage 3 cells, Kif1A^{cc} accumulated at the tips of nearly all minor neurites (Fig. 2A). Occasionally, the fluorescence temporarily disappeared from a neurite (see neurite 5, Fig. 2C). The relative amount of Kif1A^{cc} fluorescence in different neurites was similar and remained fairly constant over time (Fig. 2C), suggesting that it translocated with roughly equal efficiency in all of the neurites.

The dynamics of Kif5C^{560} accumulation in stage 2 cells were quite different and unexpected – Kif5C^{560} concentrated in only one or two growth cones at a time (Fig. 2B). Moreover, its accumulation was transient; it disappeared from one neurite and appeared in another, sometimes within a period of 30 minutes (Fig. 2D). This difference was consistent across all cells examined (N=14 for Kif5C^{560}, 12 for Kif1A^{cc}). In Kif1A expressing cells, >80% of the tip fluorescence was concentrated in a *single* neurite in only 7 instances in a total of

315 time lapse images, whereas Kif5C^{560} fluorescence was concentrated in a single neurite in 155 out of 348 images (T-test, $p<0.001$).

When the accumulation of Kif5C^{560} fluorescence in one neurite disappeared, the total amount of fluorescence in the cell did not show a corresponding decline, but instead became diffusely distributed (Suppl. Fig. 2). Likewise the re-accumulation of Kif5C^{560} fluorescence at the tip of a different neurite was not accompanied by an increase in total fluorescence. Thus, changes in the location of Kif5C^{560} accumulations are unlikely to involve protein degradation or synthesis. Its redistribution most likely reflects its detachment from microtubules in one neurite and diffusion throughout the cell, followed by rebinding and active translocation along a different subset of microtubules. The involvement of a retrograde motor is unlikely because the construct lacks a cargo-binding domain that would allow it to associate with organelles undergoing motor-driven transport. Redistribution of such a large fraction of the cell's Kif5C^{560} fluorescence implies a coordinated change in the behavior of many Kif5C^{560} molecules. Quantitative analysis of the fluorescence distribution in the cell shown in Figure 2b showed that Kif5C^{560} successively accumulated multiple times in each of the 4 neurites during the 9-hour duration of this recording (Fig. 2D). In other cells, Kif5C^{560} accumulated repeatedly in the *same* neurite; periods of active translocation were interspersed with periods when the protein was diffusely distributed (see Figure 4B and F).

To assess the extent to which Kif5C^{560} accumulated preferentially in only a subset of neurites, we quantified the fluorescence in individual frames from

time-lapse recordings of stage 2 cells expressing Kif5C^{560} or Kif1A^{cc}, ranking the neurites from brightest to dimmest (Supp. Fig. 3). In the case of Kif5C^{560}, the brightest growth cone contained, on average, 76% of the fluorescence present in the neurites, with little fluorescence present in the remaining neurites. Kif1A^{cc} fluorescence was more evenly distributed among all the neurites; this difference was highly significant ($p < 0.001$).

During developmental stage 2, neurites undergo periods of growth followed by periods of retraction in an apparently stochastic pattern (gray traces in Fig.4), as described previously (Esch et al., 1999). To determine whether the transient accumulations of Kif5C^{560} correlated with these stochastic growth events, we quantified the growth and retraction of each neurite and the Kif5C^{560} fluorescence in each growth cone in recordings of 12 stage 2 cells over a combined total of 72 hours of recording (Fig. 3). Large increases in Kif5C^{560} fluorescence were as likely to be associated with a retraction as with an elongation (mean length change: -0.07 μm; Fig. 3A). Nor was there a correlation between neurite growth and the fraction of Kif5C^{560} fluorescence present in a given neurite ($r = -0.13$; Fig. 3B). We conclude that the accumulation of Kif5C^{560} in a given neurite's growth cone is not related to the growth of that neurite.

Taken together, these results imply that there are transient biochemical differences among the neurites of stage 2 cells and that the motor domain of Kif5C, but not that of Kif1A, recognizes these differences. Whatever the nature of these differences, they must be rapidly modifiable, because Kif5C^{560} sometimes redistributed from one neurite to another in as little as 30 minutes.

The stable accumulation of truncated Kinesin-1 in a single neurite is an early marker of axon specification.

To examine the localization of Kif5C^{560} during axon specification, we acquired time-lapse images of Kif5C^{560}-expressing neurons during the transition from stage 2 to 3. Figures 4A and B show selected images from recordings of two representative neurons; quantification of changes in the distribution of Kif5C^{560} fluorescence in these cells is shown in Figures 4C and D. In the cell shown in Fig. 4A, Kif5C^{560} first concentrated in one neurite tip, appeared diffusely distributed for a brief period, then re-accumulated in another neurite tip, and so on. As soon as the axon began its characteristic growth spurt, Kif5C^{560} became concentrated in the growth cone of the emerging axon and no longer appeared in any other neurite. In the cell shown in Figure 4B, Kif5C^{560} translocated repeatedly into the same neurite, with short intervening periods when it was diffusely distributed. As that neurite underwent the period of uninterrupted growth associated with its specification as the axon, Kif5C^{560} remained *stably* concentrated at its tip. Similar experiments with cells expressing Kif1A^{cc} showed that the motor accumulated at the tips of most minor neurites during stage 2 and remained concentrated in these tips, including the one that became the axon (data not shown).

We next considered the temporal relationship between the selective and stable accumulation of Kif5C^{560} in a single neurite and axon specification. Clearly, the accumulation of Kif5C^{560} in a single neurite does not predict that it will become the axon. In some cells at developmental stage 2, Kif5C^{560} transiently

accumulated in neurites that did not become the axon (Fig. 4A). Instead, our observations indicate that the *stable* accumulation of $Kif5C^{560}$ in a neurite marks its specification as the axon. Fig 4E and F illustrate the temporal relationship between axon outgrowth and the stable accumulation of $Kif5C^{560}$. $Kif5C^{560}$ accumulated and remained at the tip of the nascent axon before that neurite was significantly longer or in any way morphologically distinguishable from the other neurites (Fig. 4A, 9:45; Fig. 4B, 15:30). Time-lapse observations indicate that only after a neurite becomes >15 μm longer than any other does it have a high probability of becoming the axon (T. Esch and G. Banker, unpub. obs.). For every axon formation event that we captured (N = 4), the majority of $Kif5C^{560}$ fluorescence became stably associated with the nascent axon at or before the time that neurite exceeded the 15 μm length threshold (range: -1 to 15 μm). Thus, the persistent accumulation of $Kif5C^{560}$ is a very early marker of axonal identity; it occurs well before the axon can be distinguished based on its length.

Discussion

The selective translocation of the Kinesin-1 motor domain in axons

Our results show that the motor domain of Kinesin-1 ($Kif5C^{560}$) selectively accumulates in axons but not dendrites, and that its exclusion from dendrites is independent of their mixed microtubule polarity. The differential translocation efficiency of the Kinesin-1 motor domain must reflect a difference

in the motor-microtubule interaction in axons as compared to dendrites. It is difficult to imagine that this compartment-specific regulation of the motor-microtubule interaction involves a modification to the motor itself as there is no evidence that the Kinesin-1 motor and dimerization domains that we expressed are targets for posttranslational modification (Hollenbeck, 1993; Mallik and Gross, 2004). On the other hand, it is well known that axonal and dendritic microtubules contain different microtubule-associated proteins (MAPs), which are also differentially phosphorylated in the two regions. Furthermore, taxol abolishes the selectivity of the Kinesin-1 motor domain for the axon (Nakata and Hirokawa, 2003). This finding also favors the interpretation that the selectivity of Kinesin-1 depends on microtubule modifications because taxol interferes with microtubule dynamics and leads to changes in MAP binding and in tubulin and MAP phosphorylation (Samsonov et al., 2004).

A number of modifications to microtubules are known to alter the efficiency of motor translocation. *In vitro* binding studies show that posttranslational polyglutamylation of tubulin can regulate the affinity of Kinesin-1 for microtubules (Boucher et al., 1994). Single kinesin motility assays show that binding of MAPs reduces the rate of Kinesin-1 attachment to microtubules without affecting its velocity or run length (Seitz et al., 2002). It remains to be determined whether known differences in axonal and dendritic MAPs, or yet-to-be identified differences in post-translational modifications of tubulin, could account for enhanced translocation of the Kinesin-1 motor domain in axons.

Our results also show that the Kinesin-1 and Kinesin-3 motor domains differentially recognize different microtubule tracks within neurons. This result is surprising, because the motor domains of the two proteins are highly homologous. The only conspicuous difference between the two is the presence of a lysine loop in the microtubule binding domain of Kif1A, which may contribute to this motor's greater run length in *in vitro* motility assays (Tomishige et al., 2002). Biochemical modifications of different microtubule populations may serve to amplify small differences in the biophysical properties of different kinesins to direct them to distinct subcellular destinations. For example, if MAPs associated with dendritic microtubules reduce the affinity of both kinesins, the greater processivity of Kinesin-3 may compensate for this, accounting for its ability to accumulate in dendrites when Kinesin-1 cannot.

The role of kinesins in the development of neuronal polarity.

During developmental stage 2, all neurites have been thought to be morphologically and molecularly identical. When one neurite stood out as having some axonal feature – a large growth cone or a higher concentration of an axonal protein – this asymmetry was interpreted as an indication that the unique neurite was about to become the axon. Much to our surprise, this view is incorrect. Using Kinesin-1 as an indicator, our results show that molecular differences among stage 2 neurites arise transiently *long* before the emergence of the axon. These differences can change rapidly, often appearing and then disappearing from a neurite within an hour. It will be important to determine if other axonal markers

also transiently label some stage 2 neurites and whether they mark the same neurites that show an accumulation of Kinesin-1.

The persistent accumulation of Kinesin-1 in a single neurite is one of the earliest known markers of axonal identity. Classical polarity markers, such as MAPs, become differentially distributed only after the axon has become significantly longer than the remaining minor neurites (Boyne et al., 1995; Mandell and Banker, 1996). Equally important, the accumulation of Kinesin-1 can be monitored in real time. Several proteins have been proposed as early makers of axon identity based on their restriction to a single neurite in *fixed* stage 2 cells (Da Silva et al., 2005; Schwamborn and Puschel, 2004). Our results demonstrate the limitations of this approach. A "snapshot" of a Kinesin-1-expressing neuron at stage 2 would often show that the motor had accumulated in a single growth cone, but this neurite does not necessarily go on to become the axon.

The selectivity of Kinesin-1 translocation early in axon specification could ensure that Kinesin-1 cargoes are targeted to just one neurite. One Kinesin-1 cargo, CMRP2 (Kimura et al., 2005), regulates tubulin assembly at the growth cone and is required for axon growth (Inagaki et al., 2001). Another Kinesin-1 cargo, JNK-Interacting Protein (Verhey et al., 2001), is a scaffolding protein that regulates the activity of cJun-Activated Kinase, whose targets include tau and doublecortin (Chang et al., 2003; Gdalyahu et al., 2004; Reynolds et al., 1997). If these Kinesin-1 cargoes modified microtubules in a way that enhanced the

translocation of Kinesin-1, this could result in a positive feedback loop that contributed to the further differentiation of the axon.

Jiang and Rao (2005) have raised the question of whether the same molecular mechanisms regulate molecular differentiation of the axon and axon growth. Because the axon is often defined by its greater length, it is difficult to distinguish these two components of axon specification. During stage 2 we found no correlation between the minor neurites undergoing growth spurts and those with accumulations of Kinesin-1. This finding suggests that the signaling events that lead to minor neurite elongation are different from those that lead to enhanced translocation of Kinesin-1, suggesting that at this stage growth and molecular differentiation are indeed separable events. One hallmark of stage 2 neurons is that their neurites undergo cycles of growth and retraction. What distinguishes the growth event that persists to generate the definitive axon? If the signaling events that regulate neurite elongation and molecular specification are independent, they may occur stochastically in different minor neurites. When, by chance, these distinct signaling events occur simultaneously in a single neurite, it may become the axon.

Acknowledgments

We are grateful to Julie Luisi-Harp and Barbara Smoody for technical assistance, to Stefanie Kaech Petrie for assistance with microscopy and analysis, and to the entire Banker Lab for insightful feedback. This research was supported by NIH grants NS17112 and MH66179 (to GB) and by NRSA Fellowship NS488655 (to CS).

Experimental Procedures

DNA Constructs

The following constructs were prepared by PCR and subcloned into the expression vector pJPA5 (J. Adelman, Oregon Health and Science University) that had been modified to include YFP: Kif5C-560-YFP (aa 1-560 of rat Kif5C; provided by B. Schnapp); Kif5C-G235A-YFP (point mutation at position 235); Kif5C-339-YFP (aa 1-339); YFP-Kif5C (full-length); Kif1A-5C-YFP (aa 1-363 of rat Kif1A, provided by B. Schnapp, aa 334-560 of rat Kif5C); Kif1A-5C-G251A-YFP (point mutation at position 251); Kif1A-396-YFP (aa 1-396); Kif1A-360-YFP (aa 1-360). The ATP hydrolysis mutants (Kif5C-G235A-YFP, Kif1A-5C-G251A-YFP) were made by PCR-based site-directed mutagenesis. For live imaging studies, Kif5C-560-YFP and Kif1A-5C-YFP were amplified by PCR from the above constructs and inserted into the expression vector p-beta-actin (S. Impey). All sequences were confirmed by restriction enzyme analysis and dideoxynucleotide sequencing.

Cell Culture

Primary hippocampal cultures with glial feeder layers were prepared from E18 embryonic rats as described previously (Goslin et al, 1998). Briefly, dissociated neurons were plated onto poly-L-lysine-treated glass coverslips at a density of 50–100 cells/mm2 and cocultured over a monolayer of astrocytes. Cells were maintained in N2.1 medium (LifeTech/GIBCO-BRL, Gaithersburg, MD).

Transfection

For fixed cell experiments, cells were transfected with Lipofectamine 2000 after 48 hours (developmental stage 3) in culture, using a total of 2-3 μg of plasmid DNA per 6 cm dish culture. Six hours after transfection, cells were fixed in PBS containing 4% paraformaldehyde and 0.4% sucrose for 20 minutes at room temperature. For live imaging experiments, cells were electroporated using a Nucleofector I (amaxa Inc., Gaithersburg, MD) with 2-3μg of plasmid DNA per 500K cells before plating. Live imaging experiments began 24-48 hours after plating.

Quantitative Analysis

For the fixed cell data obtained from stage 3 neurons, accumulation in a neurite tip was defined as a fluorescence intensity ratio of greater than six between the neurite tip and the corresponding shaft. We used the threshold function in Metamorph to exclude background fluorescence. We compared the average pixel intensity of equal regions in a neurite's tip and its shaft. A soluble protein results in a tip:shaft fluorescence intensity ratio of approx. 1.5, which reflects a difference in volume between the two domains. Thus, a fluorescence intensity ratio of 6 reflects a ~4-fold difference in concentration of the motor protein. 80-100 neurites from 21-24 cells from 3 experiments were analyzed for each construct.

For the bright-dim bar graph of stage 2 cells, 10-11 cells were analyzed at two different time points for each construct. After subtracting background

fluorescence, the fluorescence intensity from the brightest to the dimmest growth cones was averaged.

Live imaging

All imaging was done on a Leica microscope and digital images acquired using a Princeton Instruments Micromax CCD camera (Roper Scientific, Trenton, NJ) controlled by MetaMorph image acquisition and analysis software (Universal Imaging Company, Downingtown, PA). Coverslips were sealed into a heated chamber (Warner Instruments, Hamden, CT) containing glia-conditioned medium without phenol red. Cells were maintained at 32°C for the duration of the recording. Neurons were imaged both at developmental stage 2 (24 hours after plating) and at developmental stage 3 (48 hours after plating). Four to six transfected neurons from each coverslip were chosen for time-lapse imaging. Every 15 minutes, a phase contrast image and a 500ms exposure fluorescence image of each cell were acquired. In some cases, although the cells appeared to be viable, fluorescence distribution retreated exclusively to the cell body for prolonged periods of time, without intermittently appearing at neurite tips. In these cases, the recording was stopped before apparent cell death and the ends of these recordings were not included in analysis.

Figure Legends

Figure 1 **Truncated Kinesin-1 selectively accumulates in the axon before the appearance of minus end-out microtubules in dendrites. A,** Kif5C^{560} consisted of the motor, neck linker, neck coil, and stalk1 domains of Kinesin-1 (amino acids 1-560) fused to YFP. Kif1A^{396}, consisted of the motor, neck linker and neck coil domains of Kinesin-3 (amino acids 1-396) fused to YFP. KIF1A^{cc} consisted of the motor and neck linker regions of Kinesin-3 (1-363) and the neck coil and dimerization domains of Kinesin-1 (337-560) fused to YFP. **B**, At stage 3, Kif5C^{560} accumulated only at the ends of the axon, whereas Kif1A^{396} accumulated at the ends of both axons and immature dendrites. In these experiments, 2-day old neurons were co-transfected with either Kif5C^{560} or Kif1A^{396} together with soluble CFP to illustrate cell morphology, and then fixed 6h later. Overlay images show soluble CFP pseudo-colored in green and the YFP-tagged motor in red. Arrows, dendrites; arrowheads, axons. Scale bars: 10μm.

Figure 2 **Truncated Kinesin-1 selectively translocates into different neurites at stage 2, before an axon has formed.** **A** and **B** show selected frames from time-lapse recordings of stage 2 neurons expressing Kif1A^{cc} or Kif5C^{560}, respectively; the entire recordings are shown in supplementary movies 1 & 2. The top panels show the fluorescence images of each motor overlaid on the corresponding phase contrast images (to illustrate cell morphology); fluorescence images alone are shown in the bottom panels. Kif1A^{cc} fluorescence remained concentrated in the tips of most neurites throughout the entire recording period

and was fairly evenly distributed among the different growth cones. In marked contrast, Kif5C^{560} accumulated in only one growth cone at a time. In the interval illustrated (1.25h), Kif5C^{560} sequentially translocated into 3 different neurites. **C** and **D** quantify the percentage of total cell fluorescence of the truncated motors present in the cells shown in **A** and **B**, respectively. In these experiments, cells were electroporated with constructs encoding either Kif1A^{cc}-YFP or Kif5C^{560}-YFP at the time of plating. Imaging began 24 hours later. Phase contrast and fluorescence images were taken every 15 minutes. Scale bars: 25 μm.

Figure 3 **Kinesin-1 accumulation does not correlate with minor neurite growth during developmental stage 2.** **A,** For every 30 minute period, each increase of fluorescence greater than 20% in a given neurite tip was plotted against the concurrent change in length of that neurite (N=89). For every non-zero change in length that accompanied an increase in fluorescence, 46% were growth events and 54% were retractions. **B,** For every positive increase in length over each 30 minute period, we examined the fraction of total fluorescence present at the tip of the growing neurite at the end of that period. There was no correlation between growth and Kif5C560 accumulation ($r = -0.13$; $N = 672$). Note that many substantial increases in length were not accompanied by the presence of a large amount of fluorescence (right side of graph).

Figure 4 **The selective translocation of truncated Kinesin-1 into the nascent axon is an early event during the specification of neuronal polarity.** **A** and **B** show Kif5C^{560} fluorescence overlaid on the corresponding phase contrast images of two cells undergoing the transition from developmental stage 2 to stage 3, when identity of the axon is first specified. **C** and **D** quantify the distribution of Kif5C^{560} fluorescence in the cells shown in **A** and **B**, respectively. **E** and **F** show the temporal relationship between neurite growth and the accumulation of Kif5C^{560} in the nascent axon. In these experiments, neurons were electroporated with a construct encoding truncated Kif5C^{560}-YFP at the time of plating. Imaging began 24 hours later. Phase contrast and fluorescence images were taken every 15 minutes. The entire recordings are shown in supplemental movies 4 & 5. Scale bars: 25μm.

Supplemental Figure 1 **Truncated Kinesin-1 accumulates at the ends of neurites due to its own active translocation.** **A** and **B,** The majority of both endogenous Kinesin-1 and full-length, expressed YFP-tagged Kif5C are evenly distributed throughout the neuron (similar to any soluble protein). This is expected because only a small fraction of the Kinesin-1 within a cell is bound to microtubules and actively translocating at any given time. **C**, In contrast, the constitutively active, truncated Kif5C^{560}-YFP accumulates at the ends of the axon. **D,** A point mutation in the ATPase domain of Kif5C^{560} prevents its accumulation in axonal growth cones. Instead, the mutant motor decorates microtubules in the cell body and proximal neurites. **E**, A construct consisting of the motor and neck

linker domains of Kif5C, which is a monomer and therefore not processive, also failed to accumulate in axon tips, and instead appeared soluble.

Supplemental Figure 2 **The loss of truncated Kinesin-1 from the tip of a neurite reflects redistribution, not degradation**. This figure shows the absolute fluorescence levels in one neurite and the cell body along with the cell's total fluorescence. In this cell, $Kif5C^{560}$-YFP underwent repeated periods of accumulation in the single neurite illustrated followed by periods of diffuse distribution, when most of the fluorescence was present in the cell body, due to its large volume. During the period shown, although the neurite's level of fluorescence decreased abruptly multiple times (red), the **total** amount of fluorescence in the cell (black) did not drastically change. As the fluorescence left the neurite, it appeared in the cell body (gray). The total levels of fluorescence slowly decreased over time most likely due to photo bleaching or a decrease in expression levels of the transgene.

Supplemental Figure 3 **The motor domain of Kinesin-1, but not that of Kinesin-3, accumulates preferentially in one or two neurites at a time.** This figure shows the fraction of total growth cone fluorescence present in the tip of each neurite, ranked from the brightest to the dimmest. In neurons transfected with $Kif5C^{560}$, the vast majority of fluorescence was concentrated in a single growth cone. In neurons transfected with $Kif1A^{cc}$, was more evenly distributed among all the neurites; the brightest neurite contained a much lower fraction of

the fluorescence (T-test, $p<0.001$). These data are based on random frames from recordings of 11-14 cells for each construct.

Supplemental movie 1 **Kif1A^{cc}-YFP accumulates at the ends of all neurites during developmental stage 3.** This neuron was electroporated at time of plating and imaging began 48 hours later. Phase and fluorescence images were acquired every 10 minutes. The movie shows 2 frames every second.

Supplemental movie 2 **Kif1A^{cc}-YFP accumulates at the ends of all neurites during developmental stage 2.** This neuron was electroporated at time of plating and imaging began 24 hours later. Phase images and fluorescence images were acquired every 15 minutes. The movie shows the fluorescence images at 2 frames every second.

Supplemental movie 3 **Kif1A^{cc}-YFP accumulates at the ends of all neurites during developmental stage 2.** This movie shows the fluorescence images overlaid onto the corresponding phase contrast images of the cell shown in Supplemental Movie 2 to illustrate cell morphology.

Supplemental movie 4 **Kif5C^{560}-YFP selectively translocates into different during developmental stage 2.** This neuron was electroporated at time of plating and imaging began 24 hours later. Phase and fluorescence images were acquired every 15 minutes. The movie shows the fluorescence images at 2 frames every

second. In this cell, the accumulation of Kif5C^{560}-YFP appears to move back toward the cell body as a bolus. This behavior was the exception rather than the rule. In most cases (120 out of 149), the fluorescence simply disappeared from the neurite tip and became evenly distributed throughout the cell (see suppl. movies 7 and 9).

Supplemental movie 5 **Kif5C^{560}-YFP selectively translocates into different during developmental stage 2.** This movie shows the fluorescence images overlaid onto the corresponding phase contrast images of the cell shown in Supplemental Movie 4 to illustrate cell morphology.

Supplemental movie 6 & 8 **The stable accumulation of Kif5C^{560}-YFP in one neurite coincides with its specification as the axon.** This neuron was electroporated at time of plating and imaging began 24 hours later. Phase and fluorescence images were acquired every 15 minutes. Fluorescence images are shown at 2 frames per second.

Supplemental movies 7& 9 **The stable accumulation of Kif5C^{560}-YFP in one neurite coincides with its specification as the axon.** These movies shows the fluorescence images overlaid onto the corresponding phase contrast images of the cells shown in Supplemental Movie 6 & 8, respectively, to illustrate cell morphology.

Figure 1

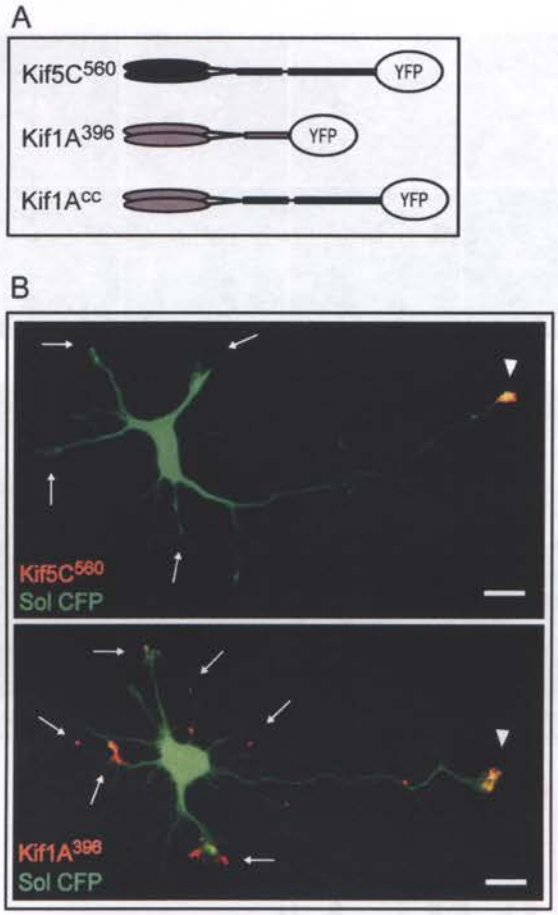
A
Kif5C560
YFP
Kif1A396
YFP
Kif1Acc
YFP
B
Kif5C560
Sol CFP
Kif1A396
Sol CFP

Figure 2

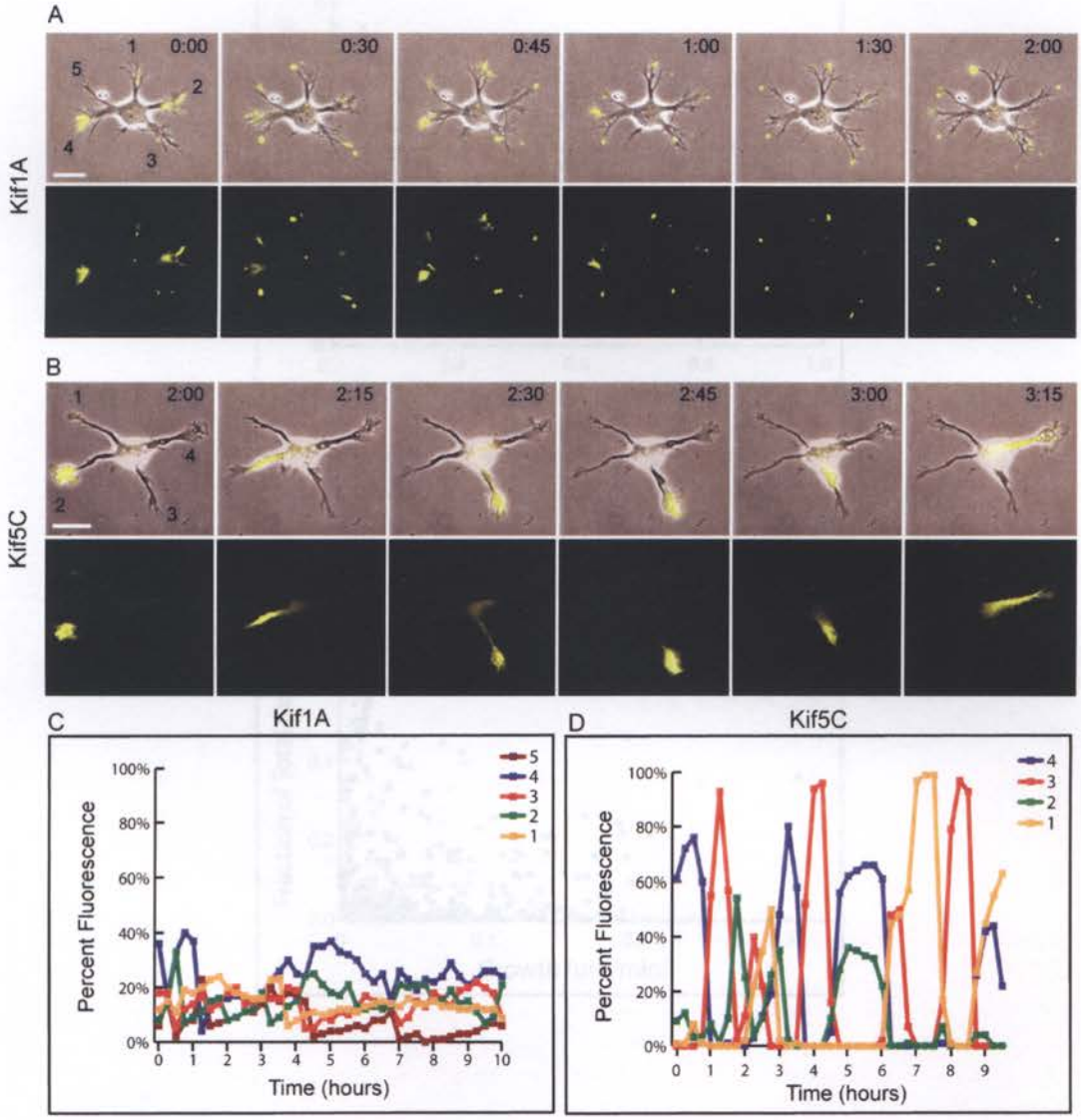
A
Kif1A
1
0:00
0:30
0:45
1:00
1:30
2:00
5
2
4
3
B
Kif5C
1
2:00
2:15
2:30
2:45
3:00
3:15
4
2
3
C
Kif1A
Percent Fluorescence
100%
80%
60%
40%
20%
0%
0 1 2 3 4 5 6 7 8 9 10
Time (hours)
5
4
3
2
1
D
Kif5C
Percent Fluorescence
100%
80%
60%
40%
20%
0%
0 1 2 3 4 5 6 7 8 9
Time (hours)
4
3
2
1

Figure 3

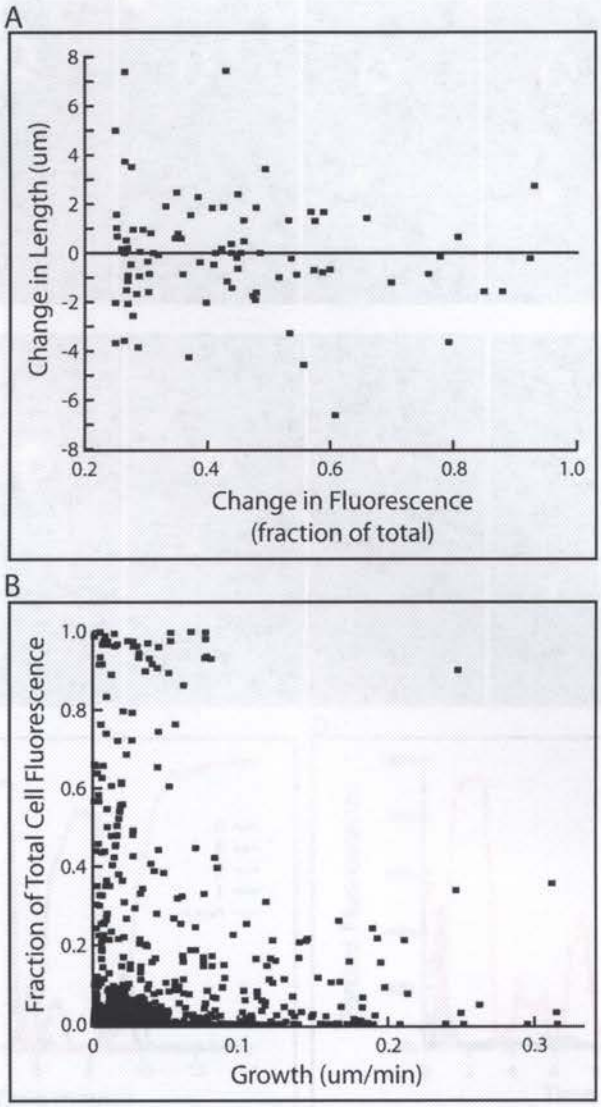
A
Change in Length (um)
8
6
4
2
0
-2
-4
-6
-8
0.2
0.4
0.6
0.8
1.0
Change in Fluorescence
(fraction of total)
B
Fraction of Total Cell Fluorescence
1.0
0.8
0.6
0.4
0.2
0.0
0
0.1
0.2
0.3
Growth (um/min)

Figure 4

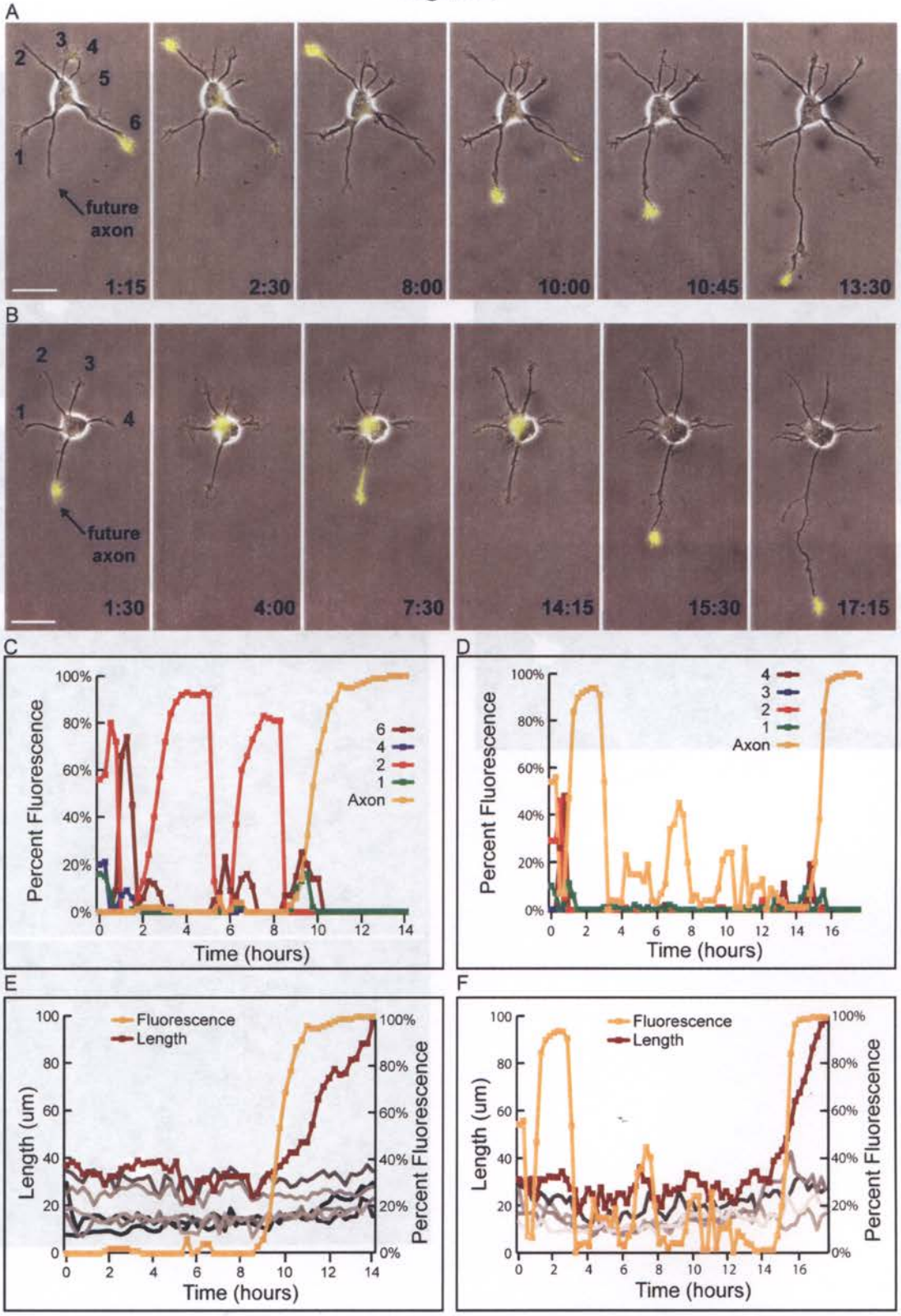
A
1
2
3
4
5
6
future axon
1:15
2:30
8:00
10:00
10:45
13:30
B
1
2
3
4
future axon
1:30
4:00
7:30
14:15
15:30
17:15
C
Percent Fluorescence
100%
80%
60%
40%
20%
0%
0
2
4
6
8
10
12
14
Time (hours)
6
4
2
1
Axon
D
Percent Fluorescence
100%
80%
60%
40%
20%
0%
0
2
4
6
8
10
12
14
16
Time (hours)
4
3
2
1
Axon
E
Length (um)
Percent Fluorescence
Fluorescence
Length
100
80
60
40
20
0
100%
80%
60%
40%
20%
0%
0
2
4
6
8
10
12
14
Time (hours)
F
Length (um)
Percent Fluorescence
Fluorescence
Length
100
80
60
40
20
0
100%
80%
60%
40%
20%
0%
0
2
4
6
8
10
12
14
16
Time (hours)

Supplemental Figure 1

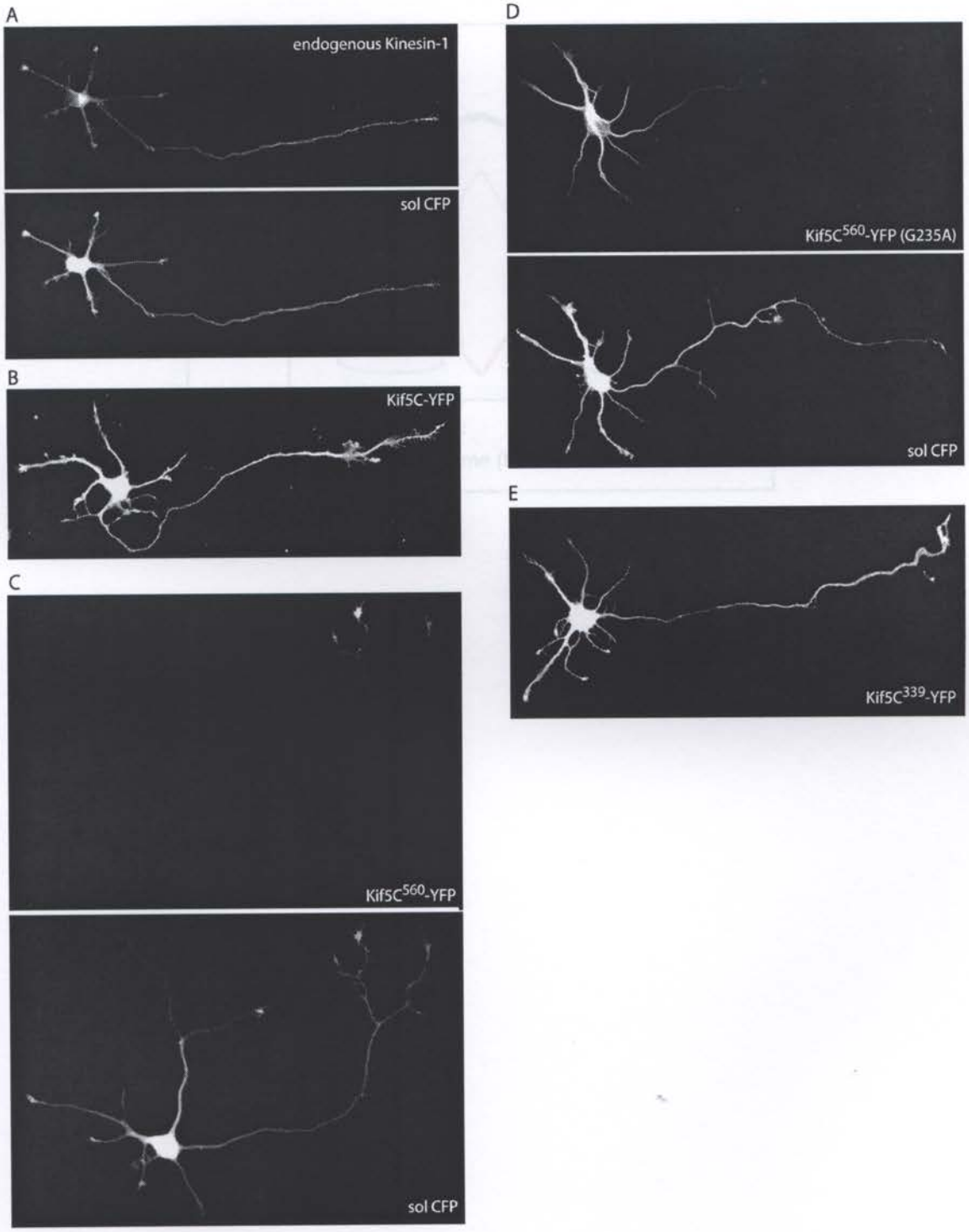

Supplemental Figure 2

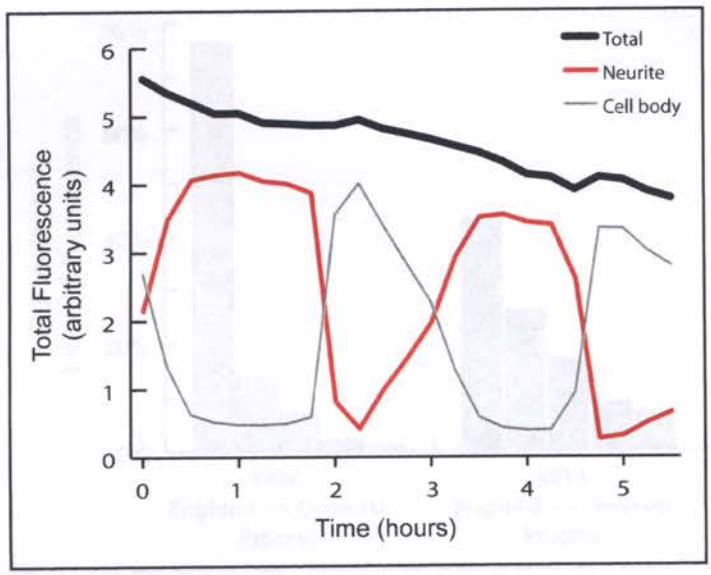

Supplemental Figure 3

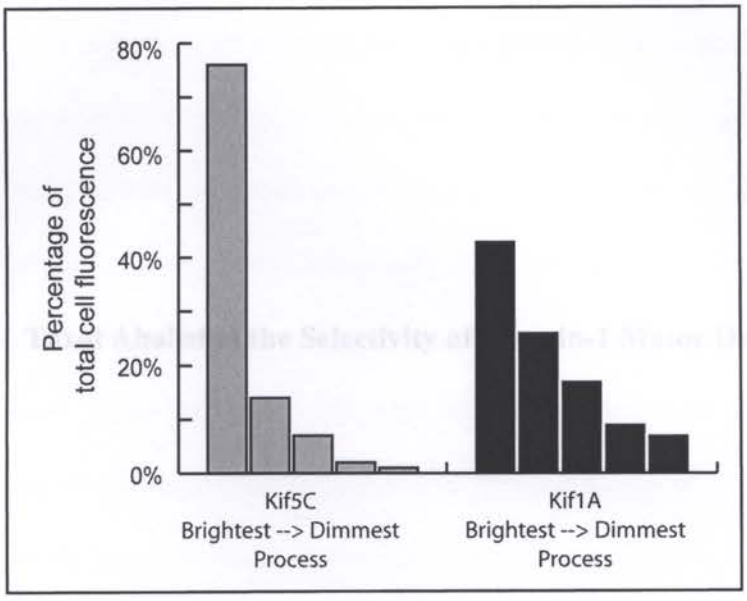

Chapter 4

Taxol Abolishes the Selectivity of Kinesin-1 Motor Domain

Catherine Selph and Gary A. Banker

[1]Center for Research on Occupational and Environmental Toxicology,

Oregon Health & Science University, Portland, OR 97239

Abstract

We tested the effects of the microtubule-stabilizing drug taxol on the selectivity of the Kinesin-1 motor domain in cultured hippocampal neurons. Live cell imaging of developing neurons revealed that, in the presence of taxol, the Kinesin-1 motor domain no longer accumulated selectively in a single neurite. This motor rapidly accumulated in all neurites in a manner consistent with its equivalent translocation in all neurites. Though taxol treatment reduced microtubule polymerization dynamics as measured by EB1-GFP, we found no significant correlation between reduced dynamics and Kif5 localization. These findings indicate that the effects of taxol on Kinesin-1 localization cannot be explained simply by a reduction in microtubule polymerization dynamics. We discuss other possible effects of taxol treatment that could explain this loss of selectivity.

Introduction

Neurons are highly polarized cells that develop two functionally and molecularly distinct domains, the axon and dendrites. To properly convey electrical and chemical signals from one neuron to another, they must transport an assortment of different proteins from their site of synthesis in the cell body to specific subcellular destinations throughout the neuron (Craig & Banker, 1994). The distribution of proteins in neurons requires microtubule-based transport mediated by molecular motors in the Kinesin Superfamily, but the underlying mechanisms of kinesin regulation are not known (Goldstein & Yang, 2000).

Kinesin-1 (Kif5) family members play a major role in cargo transport in neurons (Goldstein & Philp, 1999). The motor domain of Kif5 selectively accumulates at the tips of the axon, indicating that it preferentially translocates along a subset of microtubules that lead to this domain (Nakata & Hirokawa, 2003). This selective accumulation in the axon occurs independently of differences in microtubule polarity orientation between the two domains (Jacobson et al, 2006). This finding suggests that there are two molecularly distinct populations of microtubules in neurites, those in the axon and those in dendrites. The selective accumulation of Kif5 in axon tips could be the result of its preferential interaction with axonal microtubules, but the underlying mechanism of its selectivity remains unknown. Elucidating the nature of the differential motor-microtubule interaction in axons versus dendrites would lead to a better understanding of the regulation of kinesins in cargo transport.

The finding that the motor domain of Kif5 accumulates in the axon, but not dendrites, raises the question of how this motor chooses its track. Nakata & Hirokawa (2003) used the microtubule-stabilizing drug taxol to test whether altering microtubule dynamics changes the selectivity of Kif5. They found that application of taxol at low concentrations abolishes the selectivity of the Kif5 motor domain for the axon. When expressed in mature hippocampal neurons that had been treated with 10nM taxol, a fluorescently tagged version of the Kif5 motor domain accumulated at the tips of both axons and dendrites. In addition, a fluorescently labeled recombinant Kif5 motor domain preferentially labeled microtubules in the initial segment following detergent extraction, and this preference was abolished by taxol treatment. These results led the authors to conclude that the motor domain of Kif5 exhibits a higher affinity for stable microtubules in the initial segment of the axon. They hypothesized that in untreated neurons, chemically distinct, more stable microtubules in the initial segment attract the motor domain of Kif5, and that this preference for the initial segment would be sufficient to explain its selective distribution to the axon.

As further evidence of differences in microtubule stability between axons and dendrites, Nakata & Hirokawa (2003) examined the dynamics of EB1-GFP. EB1-GFP binds to elongating microtubules and can be used as an indicator of microtubule dynamics *in vivo* (Vaughan, 2004; 2005). Microtubules in the initial segments of axons were found to label more brightly with EB1-GFP than microtubules in dendrites. Analysis of the movements of EB1-GFP showed that there were more than twice as many anterogradely moving EB1-GFP puncta in

the axon initial segment than there were in dendrites. The authors concluded from these findings that Kif5-preferred microtubules in the initial segment could be distinguished based on their higher affinity for EB1.

The conclusions from the experiments described above, however, do not take into account what is known about the effects of taxol on EB1. Endogenous EB1, which under normal conditions is recruited to the plus ends of microtubules, loses its concentrated localization in the presence of taxol and instead becomes diffusely distributed (Morrison et al, 1998). These findings indicate that taxol reduces the number of actively polymerizing microtubules. Taken together with the finding that taxol abolishes the selectivity of Kif5, this result suggests that Kif5 translocates more efficiently on microtubules that are not actively polymerizing, which is inconsistent with the finding that the initial segment contains more moving EB1-GFP puncta.

Based on these seemingly contradictory findings, we set out to examine the effects of taxol on the localization of the Kif5 motor domain and EB1-GFP dynamics in cultured hippocampal neurons. We performed these experiments at earlier stages of development, including the stage before the appearance of an axon, since we had previously found that Kif5 exhibits selectivity before neuronal polarization. Examining the behavior of Kif5 at these earlier stages allowed us to avoid any complications in interpretation due to the differences in microtubule polarity that arise later in development. We found that taxol abolished the selectivity of the Kif5 motor domain at stage 3 of development in a manner consistent with its equal translocation in all neurites. The behavior of the Kif5

motor domain in the presence of taxol was consistent with all populations of microtubules becoming equivalent substrates for Kif5 translocation. Fluorescence associated with the motor increased gradually and to the same degree in all dendrites. Taxol treatment also abolished Kif5 selectivity at developmental stage 2, before the emergence of the axon. Under control conditions, the motor accumulated dynamically and transiently in various neurites; with taxol treatment, this dynamic behavior was lost, and Kif5 accumulated in all neurites. This effect occurred within the first 15 minutes of adding taxol. Next, we showed that distinct EB1 dynamics were not a good predictor of the localization of the Kif5 motor domain. We found that EB1 dynamics were similar in Kif5-positive and Kif5-negative neurites, both at stage 2 and at stage 3, indicating that the microtubules that attract Kif5 cannot reliably be identified based on distinct EB1 dynamics. Our findings suggest that, though taxol can change the preferential translocation of the Kif5 motor domain and by extension the interaction of the motor domain with the microtubule, this effect is independent of the changes in EB1 dynamics that taxol exerts.

Results

Taxol abolished the axonal selectivity of the Kif5C^{560}-YFP at developmental stage 3.

It was previously shown that taxol, at low concentrations, abolishes the selectivity of the Kif5 motor domain for the axon in *mature* hippocampal neurons

(Nakata & Hirokawa, 2003). As described in Chapter 2, the differential organization of microtubule polarity in axons versus dendrites of mature neurons makes it difficult to draw conclusions based on the accumulation of a plus end-directed motor such as Kif5. For this reason, we examined the effects of taxol on the selectivity of the Kif5C motor domain at stage 3, when microtubules in the axon and the dendrites are oriented in the same way (primarily plus end out).

In control cells, Kif5C^{560}-YFP brightly labeled the tip of the axon, but did not appear in dendritic growth cones (Fig. 1A; see also Jacobson et al., 2006). Treating the cells with 10nM taxol abolished the selectivity of the Kif5C motor domain for the axon; following taxol treatment for 3 hours, Kif5C^{560} fluorescence clearly concentrated in the tips of dendrites as well as the axon (Fig. 1B). Almost all of the axons of vehicle- and taxol-treated cells were brightly labeled with Kif5C^{560}-YFP (95% and 98%, respectively). Only 3% of vehicle-treated dendrites showed an accumulation of Kif5C^{560}-YFP, whereas the motor domain concentrated in 66% of taxol-treated dendrites (Fig. 1C, t-test, $p>0.001$). The degree of dendritic labeling following taxol treatment is comparable to that previously reported for the non-selective motor Kif1A^{396}-YFP at stage 3 (Jacobson et al., 2006). As described in that paper, live cell imaging of stage 3 neurons expressing Kif1A^{396}-YFP show that the growth and retraction of the relatively short dendrites probably explains why all dendrites do not show motor accumulation at any given time.

To investigate how long it takes for taxol treatment to alter the selectivity of the Kif5C motor domain, we used live cell imaging to visualize the dynamics

of its accumulation at stage 3. Figure 2A illustrates the dynamics of Kif5C^{560} accumulation in a control cell. As expected from observations of fixed cells, Kif5C^{560} fluorescence selectively and persistently accumulated at the tip of the axon; dendritic tips were never labeled (Fig. 2A). New protein that was synthesized in the cell body throughout the recording apparently made its way into the axon, where the vast majority of the fluorescence was localized (Fig. 2C). In contrast, taxol treatment led to the rapid accumulation of Kif5C^{560} fluorescence in the tips of developing dendrites (Fig. 2B). Fluorescence first became detectable in dendrite tips about 30-45 minutes after addition of taxol and increased continuously in intensity over time (Figure 2D). In each of the three stage 3 cells examined, fluorescence became visible in dendritic tips within an hour following addition of taxol.

Since the accumulation of Kif5C^{560}-YFP in neurite tips reflects the continuous binding to and translocation along microtubules that are pointing distally (Friedman & Vale, 1999; Tomishige et al., 2002; Nakata & Hirokawa, 2003; Lee et al., 2004; Jacobson et al., 2006), it is unlikely the truncated motor present in the axon can return to the cell body again. Indeed, live cell recordings of stage 3 cells that had not been treated with taxol showed that the fluorescence remained stably concentrated at the axonal growth cone, appearing neither in the shaft nor in the cell body (Fig. 2A & C). Thus, the appearance of fluorescence in the dendrite tips following taxol treatment likely reflects the non-selective translocation of newly synthesized Kif5C^{560} from the cell body to *all* neurite tips. This interpretation is consistent with the continuous rise in fluorescence that we

observed in dendrite tips. Taken together, these results suggest that taxol treatment abolishes the preferential interaction of Kif5C with axonal microtubules, allowing equal, non-selective translocation of the motor among all populations of microtubules.

Taxol suppresses the transient changes in the localization of Kif5C^{560}-YFP at stage 2.

The behavior of the Kif5C^{560} is quite different at stage 2, when it selectively accumulates in different neurites over time. As described in more detail in the previous chapter, at stage 2, Kif5C vacillates between periods of active translocation in one of many neurites and periods when it appears soluble, indicating that there are times when the motor is not binding to the microtubules at all. I next asked whether taxol affected the motor-microtubule interaction at this stage. In control neurons, Kif5C^{560}-YFP vacillates between concentrating in one or two neurite tips and appearing soluble (Fig. 3A). Quantitative analysis of the fluorescence distribution in the cell shown in Figure 3A illustrates that Kif5C^{560} successively accumulates multiple times in 4 out of the 5 neurites during the 4-hour duration of this recording (Fig. 3C). In the presence of taxol, however, the dynamic pattern of Kif5C^{560}-YFP accumulation is lost. Kif5C^{560} fluorescence concentrates in multiple neurites simultaneously and remains stably localized in these neurite tips throughout the recording (Fig. 3B). In the cell shown, about half of the cell's fluorescence is soluble at the beginning of the recording, which appears mostly in the soma because of its greater volume. Over the next 15

minutes, the soluble pool of fluorescence in the soma decreased as the fluorescence levels in each of the four neurite tips simultaneously increased (Fig. 3C). Fluorescence levels in the neurite tips increased 7-11%. From that point onward, fluorescence levels were fairly evenly distributed and remained constant throughout the duration of the recording. Interestingly, in the presence of taxol, the motor did not vacillate between periods of active translocation (as indicated by fluorescence accumulation at a tip) and periods of inactivity (soluble distribution), as in untreated cells. The fairly even distribution in all neurites, accompanied by the lack of intervening periods of soluble distribution, is consistent with the observations of the non-selective motor Kif1A^{396}-YFP in stage 2 neurons described in the previous chapter.

To assess the extent to which the dynamics of Kif5C^{560} accumulation in stage 2 cells were abolished with taxol treatment, I quantified the changes in fluorescence distribution. A significant accumulation in a single neurite was defined as an increase in fluorescence over 30 minutes that resulted in more than 50% of the cell's fluorescence in one neurite (see Methods). Such a definition would, for example, include 4 accumulation events for the cell shown in Figure 3A (labeled 1-4 in Fig. 3C). In untreated cells, I observed a significant accumulation of fluorescence 21 times in 39 hours of recording, or an average of about one event every two hours (N=10). In contrast, taxol-treated cells did not show a single instance of significant accumulation of fluorescence in 24 hours of recording (N=8).

These results show that taxol prevents the dynamic accumulation of the Kif5C motor domain in different processes at stage 2. Consistent with the results from stage 3 neurons, taxol appears to render all microtubules equal substrates for the translocation of the Kif5C motor domain. The motor never appeared soluble in the presence of taxol, which may indicate that taxol treatment increases the overall affinity of the motor for microtubules. These results also indicate that taxol exerts its effects on the interaction between the Kif5C motor domain and the microtubule within 15 minutes.

Low-dose Taxol treatment suppresses EB1 dynamics.

Higher doses of taxol (10μM) result in the dissociation of endogenous EB1 from the tips of microtubules (Morrison et al., 1998). To confirm that the 10nM taxol concentration that was sufficient to abolish Kif5C selectivity was also sufficient to reduce microtubule polymerization dynamics (i.e. dissociate EB1-GFP from microtubule tips), we examined EB1-GFP dynamics in cells that had been treated with this dose of taxol. Figure 4A shows vehicle- and taxol-treated cells expressing EB1-GFP. In the control condition, EB1 puncta were clearly visible throughout the cell. Fluorescence mostly concentrated in these puncta, as indicated by the lack of a soluble pool of fluorescence. The majority of the fluorescence present as puncta reflects the recruitment of EB1-GFP to microtubules that were actively polymerizing. taxol treatment resulted in a loss of EB1 puncta and was accompanied by a visible increase in soluble fluorescence, indicating that the number of actively polymerizing microtubules was reduced.

Individual moving EB1 puncta in the boxed regions of the vehicle- and taxol-treated cells are shown in a series of time-lapse images (Fig. 4B). Kymographs of the entire recordings of the boxed regions show that the EB1 events in the taxol-treated cell were fewer, slower and shorter (Fig. 4C). There were 37% as many anterogradely moving EB1 puncta in taxol-treated cells, and they moved at 49% of the velocity as those in control cells (Table 1). Furthermore, EB1 puncta in taxol-treated cells had excursion lengths that were about half as long as those in control cells (Table 1). Thus, the 10nM concentration of taxol that was sufficient to change the localization of Kif5C^{560} reduced microtubule dynamics as measured by EB1-GFP.

Distinct EB1 dynamics are not a reliable predictor of Kif5^{560}-YFP localization.

The finding that taxol allows the accumulation of Kif5C^{560} in dendrites as well as axons and reduced microtubule dynamics led me to ask whether neurites that showed an accumulation of Kif5C^{560} exhibited distinct reduced microtubule dynamics. To address this question, I compared EB1-GFP dynamics in Kif5C^{560}-positive and Kif5C^{560}-negative neurites both at stage 2 and at stage 3. In stage 2 cells, I co-transfected Kif5C^{560}-Tomato along with EB1-GFP in order to identify those neurites where Kif5C^{560} accumulated. I restricted analysis to cells where the motor was clearly concentrated in a single growth cone to maximize the possibility of observing any differences in EB1-GFP dynamics between Kif5C^{560}-positive and Kif5C^{560}-negative neurites. In the cell shown in Figure 5A,

Kif5C^{560}-Tomato was concentrated in the tip of a single neurite (neurite 1), while EB1-GFP was present in the cell body and all neurites. Individual moving EB1 puncta are highlighted in yellow in kymographs of the Kif5C^{560}-positive neurite (neurite 1) and two representative Kif5C^{560}-negative neurites (neurites 2 &3, Fig. 5B). Moving EB1 puncta were present in all three of these neurites. Based in analysis of 9 cells, there was no significant difference in the number of EB1-GFP movements in neurites in which Kif5C^{560} accumulated or failed to accumulate (Table 1).

At stage 3, co-transfection is not necessary to identify the Kif5C^{560}-positive neurite; 98% of axons, contain concentrated levels of Kif5^{560} fluorescence (see Chapter 3). Therefore, I simply compared EB1-GFP dynamics in the axon and the dendrites (Fig. 5C). Consistent with the results obtained at stage 2, there were no statistically significant differences between EB1-GFP movements in the axon compared to those in the dendrites (Fig. 5D; see also Table 1).

While not statistically significant, at both stages of development, the number of EB1-GFP movements was somewhat reduced in Kif5C^{560}-positive neurites compared to Kif5C^{560}-negative neurites (Table 1). I examined this trend more closely by comparing the number of EB1 events in the Kif5C^{560}-positive and Kif5C^{560}-negative neurites in the same cell. At stage 2, the Kif5C^{560}-positive neurite had the fewest moving EB1-GFP puncta in 8 out of 17 cells (47%, Fig. 5E). At stage 3, the axon had the fewest number of EB1-GFP movements in 6 out of 9 cells (66%, Fig. 5F). In a number of cases, however, one of the Kif5C^{560}-

negative neurites exhibited about the same number of EB1-GFP movements as the Kif5C^{560}-positive neurite (Figs. 5E & F). Although the Kif5C^{560}-positive neurite may exhibit slightly fewer EB1-GFP movements, this by itself is not a reliable predictor of where Kif5C^{560} accumulates.

Discussion

The experiments presented here were aimed at understanding the mechanisms underlying the selective axonal translocation of constitutively active Kif5. I found that reducing microtubule dynamics with the microtubule-stabilizing drug taxol abolished the selectivity of this kinesin. Though this result suggested that there might be a direct relationship between microtubule dynamics and Kif5C^{560}-YFP localization, the data presented in this chapter indicate that this is unlikely. Visualizing EB1-GFP to measure one aspect of microtubule dynamics revealed that they were not significantly different in Kif5-positive neurites from those in Kif5-negative neurites. Thus, microtubule dynamics, as measured by EB1-GFP, are not a reliable predictor of Kif5C^{560}-YFP localization.

Nakata & Hirokawa (2003) found that microtubules in the axon initial segment could be distinguished based on their polymerization dynamics and their increased affinity for constitutively active Kif5. Based on these findings, they suggested that microtubules in the initial segment are molecularly distinct from other microtubules in the neuron. They hypothesized that constitutively active Kif5 preferentially translocates along these molecularly distinct microtubules in

the initial segment, which are marked by increased levels of EB1-GFP. My results show that, at earlier stages of development, increased levels of EB1-GFP do not mark the microtubules that Kif5 prefers. I measured EB1-GFP dynamics in Kif5C^{560}-positive and in Kif5C^{560}-negative neurites, and found that EB1-GFP dynamics were similar in the two types of processes. In fact, the data presented here show that there may be a slight reduction in EB1-GFP dynamics in Kif5C^{560}-positive neurites compared to Kif5C^{560}-negative neurites.

How Does Taxol Abolish the Selective Translocation of Kif5?

The finding that microtubule dynamics per se cannot explain the selectivity of Kif5 raises the question of what other effects of taxol could account for its effects on Kif5 translocation. What mechanism could underlie the taxol-induced loss of selectivity?

Taxol reduces the binding of some microtubule-associated proteins (MAPs) with microtubules. Samsonov et al. (2004) showed that fluorescently labeled tau loses its colocalization with microtubules in living neurons within minutes of taxol application. The loss of microtubule-associated fluorescence is accompanied by an increase in the soluble pool of tau-GFP, indicating that tau is dissociating from microtubules and becoming soluble. In addition, biochemical microtubule pelleting assays from cultured sympathetic neurons have shown that when microtubules are polymerized in the presence of taxol, they incorporate less MAP2 (Black, 1987). Together with the finding that MAPs can negatively regulate the attachment of Kif5 to microtubules (Seitz et al, 2002), these findings

suggest a possible explanation for why taxol treatment allows the accumulation of Kif5 in dendrite tips. Taxol may cause the dissociation of MAPs, which are known to reduce the binding of Kif5 with microtubules.

Another possible explanation for the accumulation of Kif5 in dendrites in the presence of taxol involves post-translational modifications to tubulin. Taxol treatment increases levels of certain post-translational modifications, such as acetylation, detyrosination and phosphorylation (Gard & Kirschner, 1985, Gundersen et al, 1987, Mansfield & Gordon-Weeks, 1991). Post-translational modifications are known to influence Kif5's binding to microtubules (Larcher et al, 1996). Thus, taxol could be altering levels of post-translational modifications of microtubules in dendrites, which in turn could increase the binding efficiency of Kif5, resulting in its translocation along dendritic microtubules and the subsequent accumulation in their tips. In sum, a reduction in microtubule dynamics does not, of itself, seem to account for the selective translocation of constitutively active Kif5C.

Microtubule Polarity Orientation

Studies performed in the 1980's using the microtubule hook assay showed that ~90% of microtubules in neurites of stage 2 and stage 3 cultured hippocampal neurites were oriented with their plus ends distal to the cell body (Baas et al., 1988, Baas et al., 1989). The hook assay uses sheets of tubulin to decorate microtubules *in situ*. This results in microtubules that appeared to bear "hooks" when viewed in the electron microscope. The polarity of the microtubule can

then be determined based on the clockwise (or counter-clockwise) direction of hook curvature (McIntosh & Euteneuer, 1984). The margin of error of this technique allowed for the interpretation of these earlier data to mean that, in fact, all microtubules in these neurites were oriented with their plus ends distal.

The data presented here, however, argue against that interpretation. Using EB1-GFP as a marker for the plus ends of microtubules, I saw clear instances of microtubule polymerization toward the cell body. Consistent with these findings, the movements of another plus end binding protein in the EB1 family, EB3-GFP, also indicate that about ~15% of microtubule plus ends point toward the cell body (Stepanova et al., 2003). Thus, it seems likely that a small fraction of microtubules in the neurites of hippocampal neurites appear to be oriented with their plus ends proximal. The functional relevance of this fraction of microtubules remains to be identified.

Is the Selective Transport of Kif5 Cargo Required for Axon Specification?

The results presented in Chapter 3 indicate that Kif5C^{560}-YFP selectively translocates in the nascent axon as soon as it begins to emerge. This finding raises the possibility that the selective transport of Kif5 cargo into a single neurite may be important in the specification of one axon from many similar stage 2 neurites. In this chapter, I showed that taxol abolishes the selective translocation of Kif5, which raises the question of whether taxol would interfere with axon specification. If the accumulation of Kif5 is an indication of where this kinesin transports its endogenous cargo, then taxol treatment should result a loss of

selectivity of Kif5-mediated transport. If, for example, taxol treatment leads to the formation of multiple axons, this would indicate that the selective transport of Kif5 cargo into the emerging axon contributes to its specification.

Acknowledgments

We are grateful to Julie Luisi-Harp and Barbara Smoody for technical assistance, to Stefanie Kaech Petrie for assistance with microscopy and analysis, and to the entire Banker Lab for insightful feedback. This research was supported by NIH grants NS17112 and MH66179 (to GB) and by NRSA Fellowship NS488655 (to CS).

Experimental Procedures

DNA Constructs

The following constructs were prepared by PCR and subcloned into the expression vector p-beta-actin (S. Impey): Kif5C-560-YFP (aa 1-560 of rat Kif5C); Kif1A-396-YFP (aa 1-396 of rat Kif1A); EB1-GFP. All sequences were confirmed by restriction enzyme analysis and dideoxynucleotide sequencing.

Cell Culture and Transfection

Primary hippocampal cultures with glial feeder layers were prepared from E18 embryonic rats as described previously (Goslin et al, 1998). Briefly, dissociated neurons were plated onto poly-L-lysine-treated glass coverslips at a density of 50–100 cells/mm2 and cocultured over a monolayer of astrocytes. Cells were maintained in N2.1 medium (LifeTech/GIBCO-BRL, Gaithersburg, MD). Cells were electroporated at time of plating using a Nucleofector I (amaxa Inc., Gaithersburg, MD) with 2-3μg of plasmid DNA per 500K cells before plating. Live imaging experiments began 24-48 hours after plating.

Quantitative Analysis

Accumulation in a neurite tip was defined as a fluorescence intensity ratio of greater than six between the neurite tip and the corresponding shaft. We used the threshold function in Metamorph to exclude background fluorescence. We compared the average pixel intensity of equal regions in a neurite's tip and its shaft. A soluble protein results in a tip:shaft fluorescence intensity ratio of approx. 1.5, which reflects a difference in volume between the two domains.

Thus, a fluorescence intensity ratio of 6 reflects a ~4-fold difference in concentration of the motor protein.

Live imaging

All imaging was done on a Leica microscope and digital images acquired using a Princeton Instruments Micromax CCD camera (Roper Scientific, Trenton, NJ) controlled by MetaMorph image acquisition and analysis software (Universal Imaging Company, Downingtown, PA). Coverslips were sealed into a heated chamber (Warner Instruments, Hamden, CT) containing glia-conditioned medium without phenol red. Cells were maintained at 32°C for the duration of the recording. Neurons were imaged both at developmental stage 2 (24 hours after plating) and at developmental stage 3 (48 hours after plating). In some cases, 10nM taxol dissolved in DMSO was added to the imaging medium (at a dilution of 1:6000). For long-term imaging of Kif5C^{560}-YFP, four to six transfected neurons from each coverslip were chosen for time-lapse imaging. Every 15 minutes, a phase contrast image and a 500ms exposure fluorescence image of each cell were acquired. For short-term imaging of EB1-GFP, 500ms exposure fluorescence images were acquired in 2 second intervals.

Figure Legends

Figure 1 **Taxol treatment abolishes the selectivity of Kif5C^{560}.** **A,** In the control cell, Kif5C^{560} accumulated only at the ends of the axon, and was not detectable in dendrites. **B**, In contrast, Kif5C^{560} accumulated at the tips of both the axon and dendrites in a cell treated with 10nM taxol. **C,** Kif5C^{560} fluorescence concentrated in only 3% of dendrites of DMSO-treated control cells, whereas 66% of dendrites of taxol-treated cells showed significant accumulation ($p<0.01$). Kif5C^{560} fluorescence accumulated in axons of both DMSO- and taxol-treated cells (98%, DMSO axons, N=17 cells; 95%, taxol-treated axons, N=23 cells). In these experiments, neurons were electroporated at the time of plating, and fixed 48h later. Arrows, dendrites; arrowheads, axons. Scale bars: 10 μm.

Figure 2 **Fast-acting effects of Taxol treatment.** **A** and **B** show two frames from time-lapse recordings of control and taxol-treated stage 3 neurons expressing Kif5C^{560}-YFP. The entire recordings are shown in supplemental movies 1 & 2. The top panels show the fluorescence images of Kif5C^{560}-YFP. Phase images are shown in the bottom panels to illustrate cell morphology. Kif5C^{560} fluorescence remained concentrated in the tip of the axon throughout the recording, but never appeared in the dendrite tips of the control cell. In the taxol-treated cell, Kif5C^{560} fluorescence was also only localized to the axon tip at the beginning of the recording. Over time, however, fluorescence began to appear in the tips of 7 of 8 dendrites. **C** and **D** quantify the fraction of total cell fluorescence present in either the axon (gray bars) or the dendrites (black bars) of the cells shown in **A**

and **B**, respectively. Each bar represents one time point. Because the fluorescence is plotted as a *fraction* of the total fluorescence present in the tips, the relative fraction of fluorescence in the axon decreases as the fluorescence in the dendrites increases. In these experiments, cells were electroporated with Kif5C^{560}-YFP at the time of plating. Imaging began 48 hours later. Phase contrast and fluorescence images were taken every 15 minutes. Arrows, dendrites; arrowheads, axons. Time is shown in hrs:min. Scale bars: 10 μm.

Figure 3 **Taxol suppresses the transient changes in the localization of Kif5C^{560}-YFP at stage 2.** **A** and **B** show selected frames from time-lapse recordings of control and Taxol-treated stage 2 neurons expressing Kif5C^{560}-YFP. The entire recordings are shown in supplemental movies 3 & 4. The top panels show the fluorescence images. Phase images are shown in the bottom panels to illustrate cell morphology. In the control cell, Kif5C^{560} fluorescence alternated between concentrating in one or two neurites (t=0:00, t=1:30 and t= 4:15) and appearing solubly distributed throughout the cell (t=2:15). In contrast, Kif5C^{560} fluorescence in the taxol-treated cell was not selectively distributed in a single neurite. In the beginning of the recording, the majority of fluorescence appeared to be distributed in the cell body. By the first frame of the time-lapse recording (15' later), Kif5C^{560} fluorescence had accumulated in 3 of the 4 neurites. Over the next hour and a half, fluorescence increased in all neurites. **C** and **D** quantify the fraction of total cell fluorescence present in the neurite tips of the cells shown in **A** and **B**, respectively. In these experiments, cells were electroporated with

Kif5C^{560}-YFP at the time of plating. Imaging began 24 hours later. Phase contrast and fluorescence images were taken every 15 minutes. Scale bars: 10 μm.

Figure 4 **Taxol reduces the number and velocity of EB1 events.** **A** shows a control and a taxol-treated stage 3 neuron expressing EB1-GFP. Selected frames from time-lapse recordings of the boxed portion of each cell's axon are shown in **B** and **C**, respectively. The entire recordings are shown in supplemental movies 5 & 6. In the control cell, EB1-GFP appears as concentrated dots. In contrast, in the taxol-treated cell, EB1-GFP is more solubly distributed, although there are occasional EB1-GFP dots visible. Examples of anterogradely moving EB1 dots are marked by the arrows. **D,** The kymographs show all EB1 events (highlighted in yellow) that occurred in each axon during the recording period. In these experiments, neurons were electroporated with Kif5C^{560}-YFP at the time of plating. Imaging began 48 hours later. Fluorescence images were taken every 2 seconds. Scale bars: 10 μm.

Figure 5 **Distinct EB1 dynamics are not a reliable predictor of Kif5C^{560} localization.** **A** shows an overlay of the first frame of a time-lapse recording of stage 2 cell co-expressing EB1-GFP (green) and Kif5C^{560}-Tomato (red). Kif5C fluorescence is concentrated in only one neurite throughout the 45 second recording. The kymographs for the Kif5C-positive neurite and two representative Kif5C-negative neurites are shown in **B**. Individual EB1 movements are highlighted in yellow. These movements were confirmed by visual inspection of

the corresponding movie. **C** shows the first frame of a time-lapse recording of a stage 3 cell expressing EB1-GFP. The corresponding kymographs of the axon and three of the five dendrites are illustrated in **D**. The entire recordings are shown in supplemental movies 7 & 8. **E** and **F** show the number of EB1 movements per 10μm in each neurite from individual cells at stage 2 and at stage 3, respectively. Blue diamonds represent the number of EB1 movements in Kif5-negative neurites, while red diamonds represent the number of EB1 movements in the single Kif5-positive neurite of each cell. In these experiments, neurons were electroporated at the time of plating. Imaging began 24 hours later. Fluorescence images were taken every 2 seconds. Scale bars: 10 μm.

Supplemental movie 1 **Kif5C^{560}-YFP remains selectively and stably accumulated at the ends of the axon.** Under control conditions, Kif5C^{560} fluorescence only appears at the tip of the axon, never at the tips of dendrites. This neuron was electroporated at time of plating and imaging began 48 hours later. Phase and fluorescence images were acquired every 15 minutes. The movie shows fluorescence images at 2 frames per second.

Supplemental movie 2 **Kif5C^{560}-YFP remains selectively and stably accumulated at the ends of the axon.** This movie shows the fluorescence images overlaid onto the corresponding phase contrast images of the cell shown in Supplemental Movie 1 to illustrate cell morphology.

Supplemental movie 3 **Taxol abolishes the selectivity of Kif5C^{560}-YFP.** Taxol was added to the imaging medium immediately before imaging began. At the beginning of the recording, Kif5C^{560} fluorescence can only be detected in the tips of the axon. Over time, however, fluorescence associated with the motor appears in the dendrite tips. This neuron was electroporated at time of plating and imaging began 48 hours later. Phase and fluorescence images were acquired every 15 minutes. The movie shows fluorescence images at 2 frames per second.

Supplemental movie 4 **Taxol abolishes the selectivity of Kif5C^{560}-YFP.** This movie shows the phase contrast images of the cell shown in Supplemental Movie 3 to illustrate cell morphology.

Supplemental movie 5 **Kif5C^{560}-YFP selectively translocates into different during developmental stage 2.** This neuron was electroporated at time of plating and imaging began 24 hours later. Phase and fluorescence images were acquired every 15 minutes. Fluorescence images are shown at 2 frames per second.

Supplemental movie 6 **Kif5C^{560}-YFP selectively translocates into different during developmental stage 2.** This movie shows the fluorescence images overlaid onto the corresponding phase contrast images of the cell shown in Supplemental Movie 5 to illustrate cell morphology.

Supplemental movie 7 **Taxol suppresses the transient changes in the localization of Kif5C^{560}-YFP at stage 2.** This neuron was electroporated at time of plating and imaging began 24 hours later. Taxol was added to the imaging medium immediately before imaging began. Phase and fluorescence images were acquired every 15 minutes. This movie shows the fluorescence images at 2 frames per second.

Supplemental movie 8 **Taxol suppresses the transient changes in the localization of Kif5C^{560}-YFP at stage 2.** This movie shows the corresponding phase contrast images of the cell shown in Supplemental Movie 7 to illustrate cell morphology.

Supplemental movie 9 **EB1-GFP movements under control conditions.** This neuron was electroporated at time of plating and imaged 48 hours later. Fluorescence images were acquired every 2 seconds. This movies shows the acquired images in real time.

Supplemental movie 10 **Taxol reduces the number and velocity of EB1-GFP movements.** This neuron was electroporated at time of plating and imaged 48 hours later. Taxol was added to the imaging medium 15 minutes before imaging began. Fluorescence images were acquired every 2 seconds.

Supplemental movie 11 **Distinct EB1-GFP dynamics are not a reliable predictor of Kif5C^{560}-YFP localization at stage 2.** This neuron was co-electroporated with EB1-GFP and Kif5C^{560}-Tomato at time of plating. Imaging began 24 hours later. Fluorescence images of EB1-GFP were acquired every 2 seconds. This movie shows the acquired images in real time.

Supplemental movie 12 **Distinct EB1-GFP dynamics are not a reliable predictor of Kif5C^{560}-YFP localization at stage 3.** This neuron was electroporated with EB1-GFP at time of plating. Imaging began 24 hours later. Fluorescence images of EB1-GFP were acquired every 2 seconds. This movie shows the acquired images in real time.

Figure 1

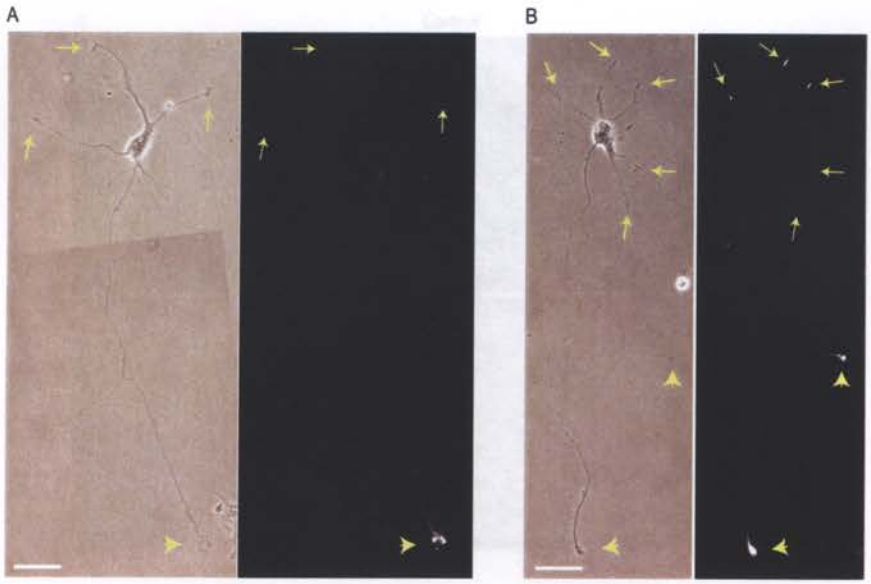
A
B

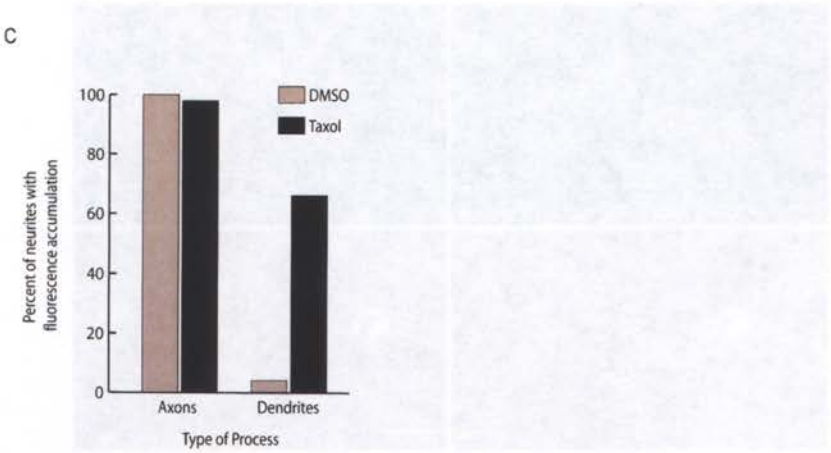
C
100
80
60
40
20
0
Percent of neurites with fluorescence accumulation
DMSO
Taxol
Axons
Dendrites
Type of Process

Figure 2

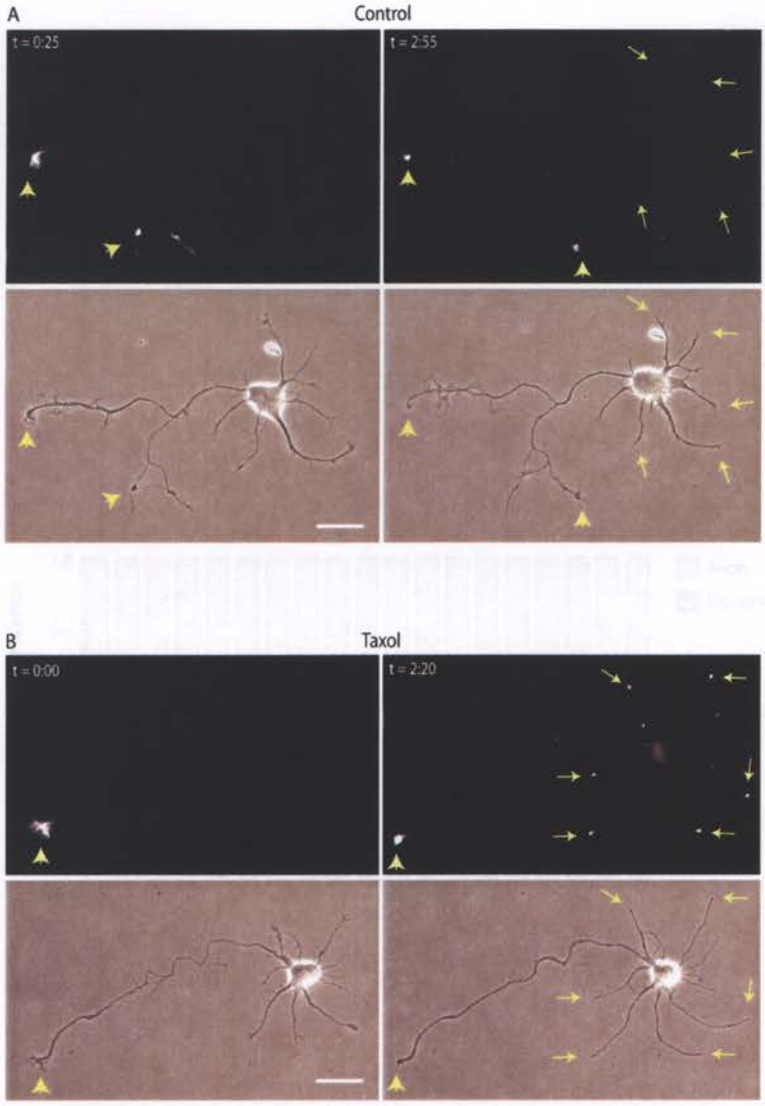

Figure 2

C

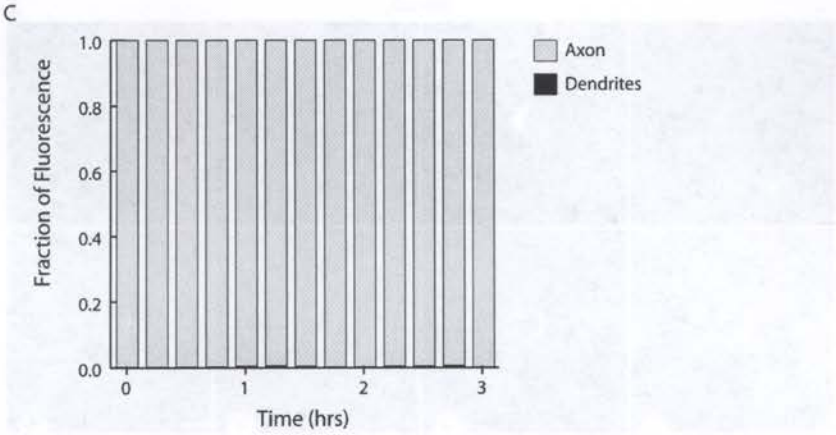
Axon
Dendrites
Fraction of Fluorescence
1.0
0.8
0.6
0.4
0.2
0.0
0
1
2
3
Time (hrs)

D

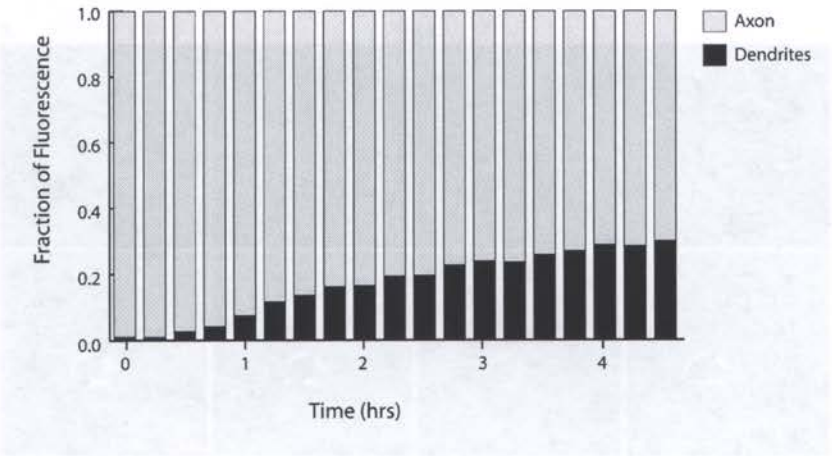
Axon
Dendrites
Fraction of Fluorescence
1.0
0.8
0.6
0.4
0.2
0.0
0
1
2
3
4
Time (hrs)

Figure 3

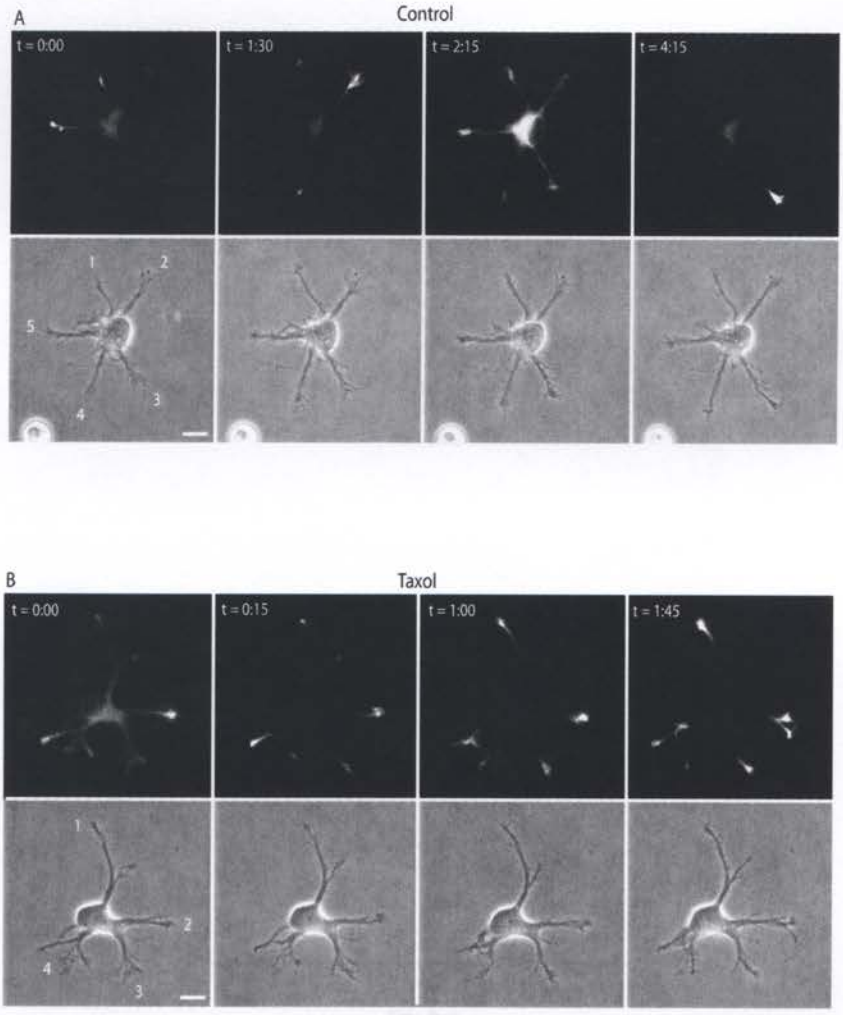
A
Control
t = 0:00
t = 1:30
t = 2:15
t = 4:15
1
2
5
3
4
B
Taxol
t = 0:00
t = 0:15
t = 1:00
t = 1:45
1
2
4
3

Figure 3

C

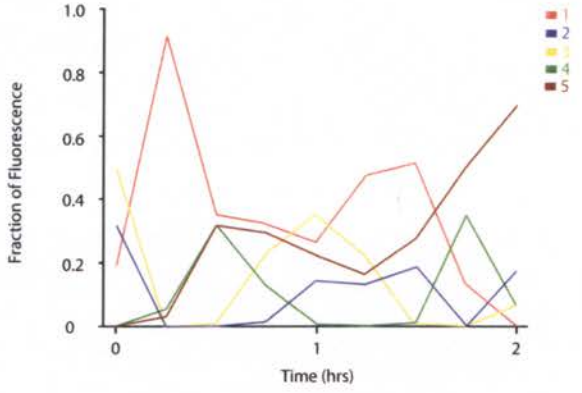
1.0
0.8
0.6
0.4
0.2
0
Fraction of Fluorescence
0
1
2
Time (hrs)
1
2
3
4
5

D

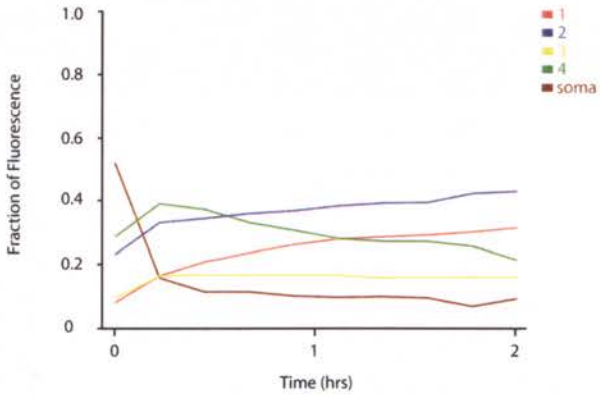
1.0
0.8
0.6
0.4
0.2
0
Fraction of Fluorescence
0
1
2
Time (hrs)
1
2
3
4
soma

Figure 4

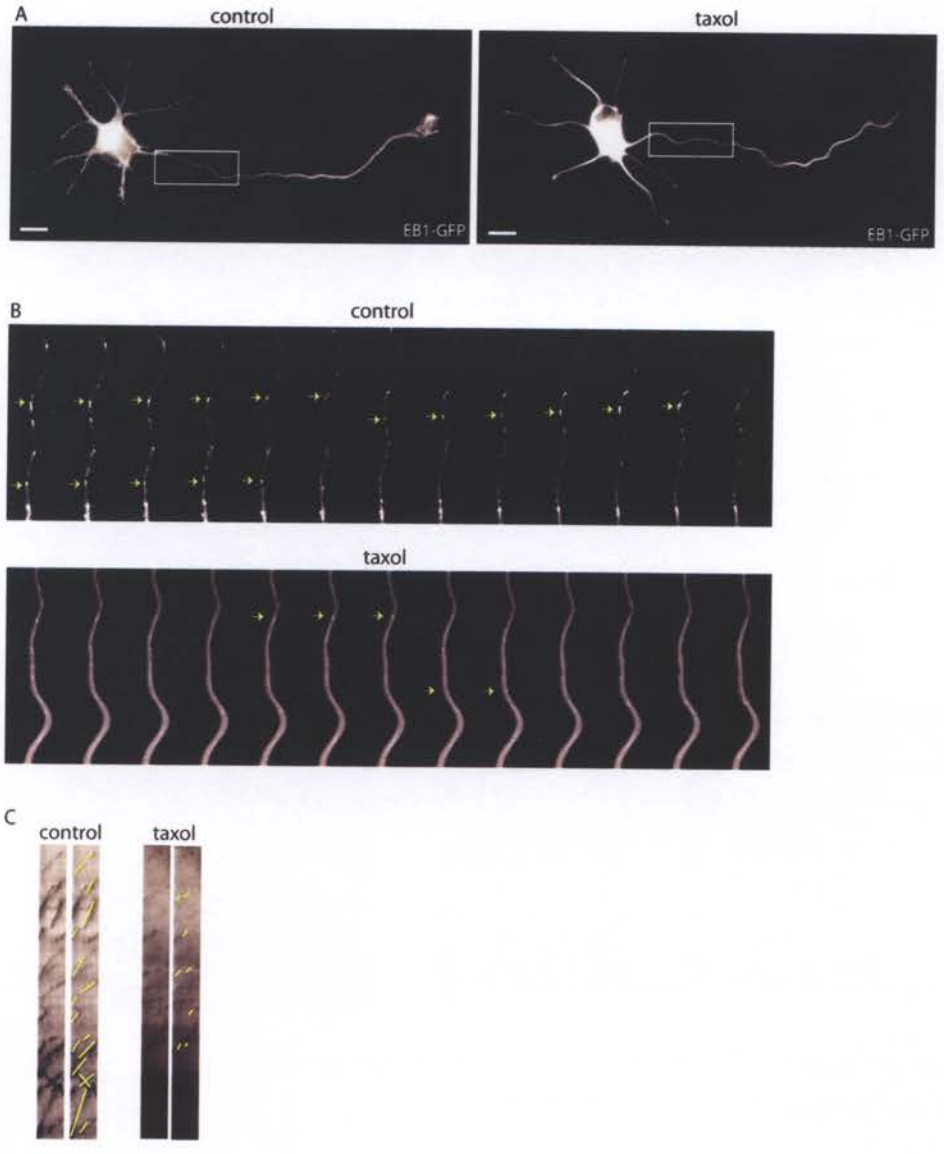
A
control
taxol
EB1-GFP
EB1-GFP
B
control
taxol
C
control
taxol

Figure 5

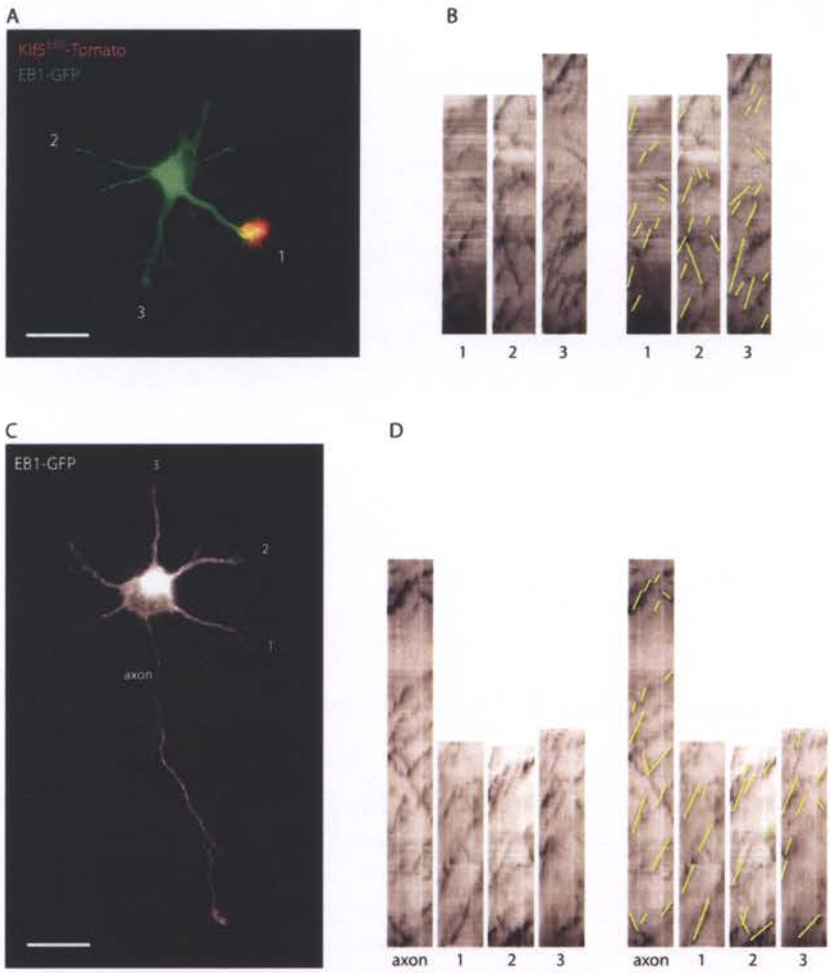
A
KIF5HD-Tomato
EB1-GFP
2
1
3
B
1 2 3 1 2 3
C
EB1-GFP
3
2
1
axon
D
axon 1 2 3
axon 1 2 3

Figure 5

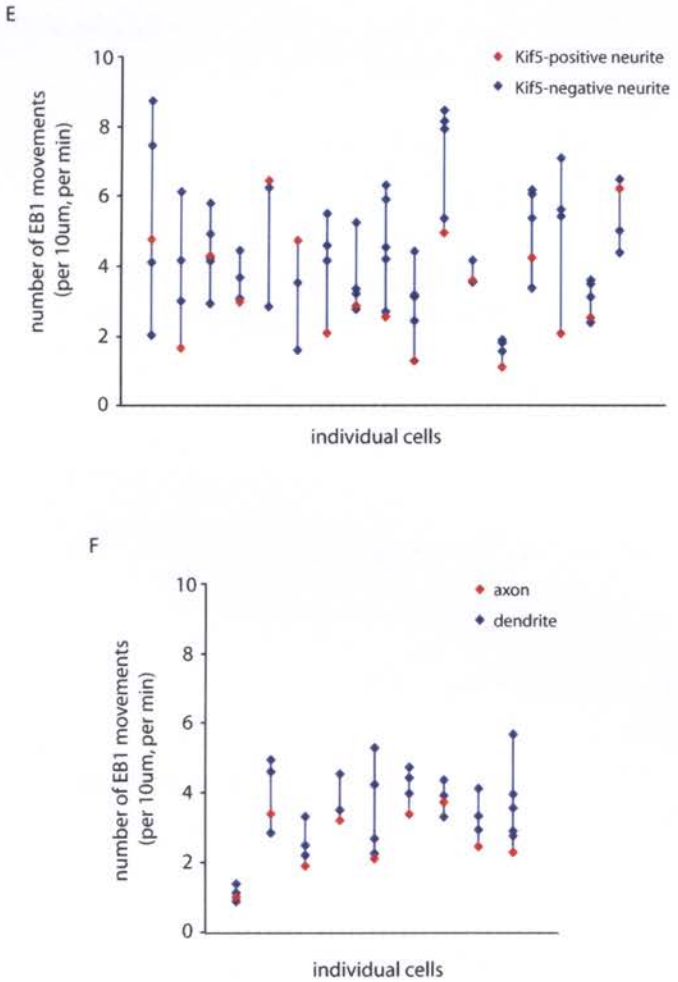
E
Kif5-positive neurite
Kif5-negative neurite
number of EB1 movements (per 10um, per min)
10
8
6
4
2
0
individual cells
F
axon
dendrite
number of EB1 movements (per 10um, per min)
10
8
6
4
2
0
individual cells

Table 1

	Number (per 10 um/per min)	Velocity (um/sec)	Duration (sec)	Excursion (um)	% Anterograde
Stage 3					
Dendrites	3.4	0.15	27	3.7	90
Axon	2.6	0.13	26	3.2	86
Axon (Taxol)	1.2	0.07	24	1.0	94
Stage 2					
Kif5-positive	3.4	0.16	24	3.6	79
Kif5-negative	4.4	0.18	20	3.0	83

Chapter 5: Discussion and Conclusions

The findings presented in the preceding two chapters suggest that the motor domain of Kif5C preferentially translocates along a subset of microtubules in neurons. In this chapter, I will discuss the future directions for this research, including experiments that could shed light on the possible mechanisms underlying this selectivity, as well as the physiological relevance of the motor's selective translocation.

Deciphering the molecular mechanism underlying the selectivity of Kif5

Single Molecule Imaging

The experiments presented in this dissertation address the question of whether Kif5 translocates along a particular subset of microtubules. The assay that was used – the accumulation of the constitutively active version – provides a clear answer to this question but gives little insight into the magnitude of the preferential translocation. Even a small difference in the efficiency of Kif5 translocation could allow it to accumulate selectively in the axon. Alternatively, it may be that this motor is completely unable to translocate in dendrites.

Kif5 motility can be described by two basic parameters: run length, which is a measure of its processivity, and attachment frequency. The lack of fluorescence in the cell body and dendrites favors the hypothesis that the attachment frequency of the motor is reduced in those domains. If the motor could still attach efficiently, but not take multiple steps, I would expect to see some low level of fluorescence throughout the cell body and dendrites. This

hypothesis is supported by studies showing that the attachment frequency, but not the run length, of Kif5 can be affected by MAPs (Seitz et al, 2002), and that certain post-translational modifications affect the binding affinity of the motor in *in vitro* studies (Larcher et al, 1996).

Visualizing the translocation of single Kif5 motors would provide data that could either strengthen or weaken this hypothesis. For example, attachment frequency and run length of single Kif5 motors in the axon could be compared to the same parameters in dendrites. If the above hypothesis is correct, the motor should exhibit fewer instances of successful attachments in the dendrites than in the axon. But there should be no differences in the run length of Kif5 in the two domains. To further test this hypothesis, these parameters could be measured in the presence of taxol, which, as Chapter 4 showed, abolished the selectivity of Kif5. A single motor imaging assay would show whether the non-selective accumulation in the presence of taxol was the result of increased attachment frequency in the dendrites.

One approach that might allow visualization of the translocation of single kinesin motors would be to increase their fluorescence levels by adding multiple GFPs. The constructs I used were tagged with one GFP; thus, each active dimer contained only two GFPs. This level of fluorescence is too low to allow visualization above the background fluorescence of the cell (pers. comm. D. Piston). Although there is the formal possibility that multiple GFPs might interfere with the translocation of the motor, this is not likely. The motor's function is to transport cargo that is attached to its tail, which is where the extra

GFP tags would reside. To increase the likelihood of being able to visualize a single motor, TIRF microscopy should be used. In this technique, only ~100nm of the cell is illuminated, which significantly decreases background fluorescence. The disadvantage to this technique is that only portion of the cell's interior is then available for fluorescence imaging. However, the processes of cultured hippocampal neurons, particularly axons, are well suited to this approach because of their small diameter (~500nm).

Microtubule Modifications

What are the microtubule modifications that result in the preferential translocation of Kif5? As discussed in Chapters 3 and 4, there are two types of modifications that have been shown to affect the interaction of Kif5 with microtubules *in vitro*: polyglutamylation of tubulin, and the association of MAPs. In this section I will discuss experiments to determine whether either of these modifications affects the translocation of Kif5 in living hippocampal neurons.

In polyglutamylation, a polyglutamate side chain of variable length is attached to a glutamate in the carboxy-terminal tail of α- and β-tubulin (Westermann & Weber, 2003). To test the role of polyglutamylation in cultured hippocampal neurons, one could express a mutant tubulin that cannot by glutamylated, at the same time blocking the expression of endogenous β-tubulin. Since Kif5 only attaches to the β-tubulin subunit, it seems more likely that modifications on this subunit would affect the motor's attachment frequency (Song & Mandelkow, 1993). If Kif5 translocated selectively in the axon because

glutamylation levels reduce its attachment frequency in dendrites, this experimental manipulation would be expected to result in the non-selective accumulation of constitutively active Kif5 in all neurites.

MAPs also reduce the attachment frequency of Kif5 to microtubules (Seitz et al., 2002). To examine the effect of MAPs on Kif5 translocation, various MAPs could be genetically knocked down. For example, examining the localization of constitutively active Kif5 in cultured hippocampal neurons from MAP2 knockout mice would resolve whether this MAP had an inhibitory effect on the translocation of Kif5. If MAP2 inhibits the attachment in dendrites, constitutively active Kif5 would be expected to accumulate at the tips of dendrites as well as axons in MAP2 knockout neurons.

In both of these cases, useful information can be obtained by examining the localization of the constitutively active version of Kif5, as in Chapters 3 and 4. However, as stated above, single molecule imaging of individual motors would provide additional insights into the mechanism underlying its selectivity.

Motor Domain Chimeras

Another approach to understanding the mechanism underlying the selectivity of Kif5 would be to exploit the fact that Kif1A is not selective. As discussed in Chapter 3, the localization of these motors was solely dependent on their motor domains. It is difficult to imagine that a microtubule modification that reduces the attachment frequency of Kif5 would not also affect the motor domain of Kif1A in a similar fashion. One possibility is that a biochemical modification

of the microtubule amplifies a small difference in the biophysical properties of these two kinesins. For example, dendritic microtubule modifications might reduce the affinity of both kinesins, but the greater processivity of Kinesin-3 may compensate for this, accounting for its ability to accumulate in dendrites when Kinesin-1 cannot.

In spite of their high homology, the two motors exhibit distinct biophysical properties, particularly in their run lengths; Kif1A has a run length that is ~10-fold longer than Kif5 (Tomishige et al., 2002). One obvious structural difference between the motor domain of Kif1A and that of Kif5C is the presence of multiple lysine residues, called the k-loop, in the neck linker region of Kif1A. The crystal structure of Kif1A indicates that this k-loop is ideally positioned to interact with the negatively charged C-terminus of tubulin (Okada et al., 1995). In addition, inserting positive charges into the neck linker region of Kif5 increases its processivity, as indicated by a longer run length (Thorn et al., 2000). Thus, one hypothesis is that these positive charges in the neck linker region of Kif1A aid this motor in overcoming a reduced attachment frequency in the dendrites by increasing its run length.

Preliminary results performed in the lab indicate that inserting a k-loop in the neck linker region of constitutively active Kif5 can indeed alter its localization pattern; like wild-type constitutively active Kif1A, this chimera accumulates at the tips of all neurites. Moreover, when the k-loop is removed from the neck linker region of Kif1A, this motor selectively accumulates in the axon tips (pers. comm. C. Huang).

Using the single motor assay to compare the translocation parameters of these various constructs would yield data that could support or oppose the hypothesis that different localization patterns are the result of differences in run length. For example, if this hypothesis is correct, both wild-type Kif1A and the Kif5 k-loop mutant should exhibit a longer run length in dendrites than wild-type Kif5 and the Kif1A k-loop deletion mutant. Moreover, the attachment frequencies of all constructs should be reduced in dendrites compared to axons.

Physiological Relevance of Selective Translocation

The data presented in this dissertation suggest that Kif5 is intrinsically targeted to a specific domain in the neuron by its preferential translocation along axonal microtubules. We do not yet know whether Kif5 preferentially transports its cargo to the axon. In this section, I will discuss experiments to address this question.

The Translocation of Full-length Kif5

As described in Chapter 3, it is not possible to visualize the transport pattern of full-length, GFP-tagged Kif5. When expressed in hippocampal neurons, this construct fills the entire cell, presumably because the majority exists as a soluble protein. One way around this technical problem would be to express a photo-activatable (PA-GFP) version. Though the entire population of PA-GFP-Kif5 would become fluorescent following photoactivating illumination of a

portion of the cell, the fluorescence due to the soluble motor would dissipate by diffusion so that the cargo-bound, translocating motor could be visualized. TIRF microscopy would further increase the signal-to-noise ratio of the photo-activated, fluorescent motor.

Visualizing the movements of full-length Kif5 would allow measurement of attachment frequency and run length. Combining these data with translocation parameters obtained from the single motor assay using constitutively active Kif5 would indicate whether the motor behaves similarly with cargo attached. This is an important point because there are some data to suggest that cargo binding can change the localization of the motor (Setou et al, 2002).

The Development of Neuronal Polarity

One of the most interesting findings presented in Chapter 3 concerned the selectivity of Kif5 during the development of neuronal polarity. Constitutively active Kif5C selectively accumulated in single neurites at stage 2. Then, as soon the nascent axon began its growth spurt, Kif5C accumulated *only* in that neurite and no longer in any other neurite. These findings raise the possibility that Kif5C is part of a positive feedback loop that contributes to the specification of the axon.

The role of Kinesin-1 in axon specification could be investigated by mistargeting the motor, and along with it, its endogenous cargo. Swapping the Kif5 motor domain with the corresponding region of Kif1A would result in a motor that translocates non-selectively in all neurites. Knocking down endogenous Kif5 using siRNA with the concomitant transfection of this Kif1A-

5C chimera into cultured hippocampal neurons should result in the non-selective transport of endogenous Kif5 cargo to all neurites. If the selective transport of endogenous Kif5 cargo is required for axon specification, this experiment should yield neurons that have multiple axons.

Visualizing Cargo Transport

Visualizing the transport of Kinesin-1 cargoes would also allow interpretations to be made about the degree of preferential transport that is physiologically relevant. For example, the experiment described above may indicate that full-length Kif5 translocates twice as many times in axons as in dendrites. Is this degree of preference physiologically relevant? The answer to this question depends on what kind of cargo Kif5 is transporting. For instance, this degree of preference may allow an unpolarized protein to be distributed evenly in both domains of the neuron – more protein must enter the axon than the dendrites because of its larger volume. However, a two-fold preference for the axonal domain may not be sufficient to result in the axonal *polarization* of a protein.

This approach depends on identifying cargoes that are transported solely by Kif5. Despite extensive research on the motor-cargo interaction, how this interaction is regulated is still largely unknown (Karcher et al, 2002). It has been shown that Kif5 can transport many different cargoes, including mRNA, protein scaffolding complexes, lysosomes and mitochondria (Vale, 2003). Additionally, in the case of mitochondria, there is some evidence that at least one other motor,

Kif1Bβ, may be involved in their transport in neurons (Nangaku et al., 1994). One way of identifying a Kif5 cargo would be to test the localization of putative Kif5 cargoes using the chimera strategy discussed above. Transfecting this chimera in the presence of siRNA constructs that knock down endogenous levels of Kif5 should result in the mislocalization of the putative cargo to dendrites.

Conclusion

In sum, this work has yielded central insights into the development of neuronal polarity as well as protein trafficking in neurons. The selective translocation of Kinesin-1 during development suggests a new model for axon specification that raises important questions about this process. Moreover, this work has led to the identification of the first axonal marker that can be used in real time to study the molecular differentiation of the axon. Pursuing the questions raised by these findings will further the understanding of these basic questions in neurobiology.

Adio, S., Reth, J., Bathe, F., and Woehlke, G. (2006). Review: regulation mechanisms of Kinesin-1. J. Muscle Res. Cell. Motil. 26, 1-8.

Aizawa, H., Sekine, Y., Takemura, R., Zhang, Z., Nangaku, M., and Hirokawa, N. (1992). Kinesin family in murine central nervous system. J. Cell Biol. 119, 1287-1296.

Al-Bassam, J., Cui, Y., Klopfenstein, D., Carragher, B. O., Vale, R. D., and Milligan, R. A. (2003). Distinct conformations of the kinesin Unc104 neck regulate a monomer to dimer motor transition. J. Cell Biol. 163, 743-753.

Allen, R. D., Metuzals, J., Tasaki, I., Brady, S. T., and Gilbert, S. P. (1982). Fast axonal transport in squid giant axon. Science 218, 1127-1129.

Amos, L. A. (1987). Kinesin from pig brain studied by electron microscopy. J. Cell Sci. 87, 105-111.

Arimura, N., and Kaibuchi, K. (2005). Key regulators in neuronal polarity. Neuron 48, 881-884.

Asbury, C. L. (2005). Kinesin: world's tiniest biped. Curr. Opin. Cell Biol. 17, 89-97.

Baas, P.W., Deitch, J.S., Black, M.M., and Banker, G.A. (1988). Polarity orientation of microtubules in hippocampal neurons: uniformity in the axon and nonuniformity in the dendrite.
Proc. Natl. Acad. Sci. USA 85, 8335-9.

Baas, P. W., Black, M. M., and Banker, G. A. (1989). Changes in microtubule polarity orientation during the development of hippocampal neurons in culture. J. Cell Biol.109, 3085-3094.

Baas, P.W., Slaughter, T., Brown, A., and Black, M.M. (1991) Microtubule dynamics in axons and dendrites. J. Neurosci. Res. 30:134-53.

Baas, P. W., and Qiang, L. (2005). Neuronal microtubules: when the MAP is the roadblock. Trends Cell Biol. 15, 183-187.

Bernstein, M., Beech, P. L., Katz, S. G., and Rosenbaum, J. L. (1994). A new kinesin-like protein (Klp1) localized to a single microtubule of the Chlamydomonas flagellum. J. Cell Biol. 125, 1313-1326.

Black, M.M. (1987) Taxol interferes with the interaction of microtubule-associated proteins with microtubules in cultured neurons. J. Neurosci. 7:3695-702.

Blair, M. A., Ma, S., and Hedera, P. (2006). Mutation in KIF5A can also cause adult-onset hereditary spastic paraplegia. Neurogenetics 7, 47-50.

Bonnet, C., Boucher, D., Lazereg, S., Pedrotti, B., Islam, K., Denoulet, P., and Larcher, J. C. (2001). Differential binding regulation of microtubule-associated proteins MAP1A, MAP1B, and MAP2 by tubulin polyglutamylation. J. Biol. Chem. 276, 12839-12848.

Bonnet, C., Denarier, E., Bosc, C., Lazereg, S., Denoulet, P., and Larcher, J. C. (2002). Interaction of STOP with neuronal tubulin is independent of polyglutamylation. Biochem. Biophys. Res. Commun. 297, 787-793.

Boucher, D., Larcher, J. C., Gros, F., and Denoulet, P. (1994). Polyglutamylation of tubulin as a progressive regulator of in vitro interactions between the microtubule-associated protein Tau and tubulin. Biochemistry 33, 12471-12477.

Boyne, L. J., Martin, K., Hockfield, S., and Fischer, I. (1995). Expression and distribution of phosphorylated MAP1B in growing axons of cultured hippocampal neurons. J. Neurosci. Res. 40, 439-450.

Bradke, F., and Dotti, C. G. (1997). Neuronal polarity: vectorial cytoplasmic flow precedes axon formation. Neuron 19, 1175-1186.

Brady, S. T., Lasek, R. J., and Allen, R. D. (1982). Fast axonal transport in extruded axoplasm from squid giant axon. Science 218, 1129-1131.

Burack, M. A., Silverman, M. A., and Banker, G. (2000). The role of selective transport in neuronal protein sorting. Neuron 26, 465-472.

Chang, L., Jones, Y., Ellisman, M. H., Goldstein, L. S., and Karin, M. (2003). JNK1 is required for maintenance of neuronal microtubules and controls phosphorylation of microtubule-associated proteins. Dev. Cell 4, 521-533.

Coy, D. L., Hancock, W. O., Wagenbach, M., and Howard, J. (1999). Kinesin's tail domain is an inhibitory regulator of the motor domain. Nat. Cell Biol. 1, 288-292.

Coy, D. L., Wagenbach, M., and Howard, J. (1999). Kinesin takes one 8-nm step for each ATP that it hydrolyzes. J. Biol. Chem. 274, 3667-3671.

Craig, A. M., and Banker, G. (1994). Neuronal polarity. Annu. Rev. Neurosci. 17, 267-310.

Dathe, V., Prols, F., and Brand-Saberi, B. (2004). Expression of kinesin kif5c during chick development. Anat. Embryol. (Berl) 207, 475-480.

Da Silva, J. S., Hasegawa, T., Miyagi, T., Dotti, C. G., and Abad-Rodriguez, J. (2005). Asymmetric membrane ganglioside sialidase activity specifies axonal fate. Nat. Neurosci. 8, 606-615.

Deitch, J.S., and Banker, G.A. (1993). An electron microscopic analysis of hippocampal neurons developing in culture: early stages in the emergence of polarity. J. Neurosci. 13, 4301-15.

Desai, A., and Mitchison, T. J. (1997). Microtubule polymerization dynamics. Annu. Rev. Cell Dev. Biol. 13, 83-117.

Dhamodharan, R., and Wadsworth, P. (1995). Modulation of microtubule dynamic instability in vivo by brain microtubule associated proteins. J. Cell Sci. 108 (Pt 4), 1679-1689.

Dotti, C. G., Sullivan, C. A., and Banker, G. A. (1988). The establishment of polarity by hippocampal neurons in culture. J. Neurosci. 8, 1454-1468.

Ebneth, A., Godemann, R., Stamer, K., Illenberger, S., Trinczek, B., and Mandelkow, E. (1998). Overexpression of tau protein inhibits kinesin-dependent trafficking of vesicles, mitochondria, and endoplasmic reticulum: implications for Alzheimer's disease. J. Cell Biol. 143, 777-794.

Esch, T., Lemmon, V., and Banker, G. (1999). Local presentation of substrate molecules directs axon specification by cultured hippocampal neurons. J. Neurosci. 19, 6417-6426.

Fichera, M., Lo Giudice, M., Falco, M., Sturnio, M., Amata, S., Calabrese, O., Bigoni, S., Calzolari, E., and Neri, M. (2004). Evidence of kinesin heavy chain (KIF5A) involvement in pure hereditary spastic paraplegia. Neurology 63, 1108-1110.

Friedman, D. S., and Vale, R. D. (1999). Single-molecule analysis of kinesin motility reveals regulation by the cargo-binding tail domain. Nat. Cell Biol. 1, 293-297.

Gard, D.L., and Kirschner, M.W. (1985). A polymer-dependent increase in phosphorylation of beta-tubulin accompanies differentiation of a mouse neuroblastoma cell line. J. Cell Biol. 100, 764-74.

Gdalyahu, A., Ghosh, I., Levy, T., Sapir, T., Sapoznik, S., Fishler, Y., Azoulai, D., and Reiner, O. (2004). DCX, a new mediator of the JNK pathway. Embo J. 23, 823-832.

Goldstein, L.S., and Philp, A.V. (1999). The road less traveled: emerging principles of kinesin motor utilization. Annu. Rev. Cell Dev. Biol.15,141-83.

Goldstein, L. S., and Yang, Z. (2000). Microtubule-based transport systems in neurons: the roles of kinesins and dyneins. Annu. Rev. Neurosci. 23, 39-71.

Goldstein, L. S. (2001). Molecular motors: from one motor many tails to one motor many tales.
Trends Cell Biol. 11, 477-482.

Goslin, K., and Banker, G. (1989). Experimental observations on the development of polarity by hippocampal neurons in culture. J. Cell Biol. 108, 1507-1516.

Goslin, K., Asmussen, H., and Banker, G. (1998). Rat hippocampal neurons in low-density culture. In Culturing Nerve Cells, G. Banker, and K. Goslin, eds. (Cambridge, MA, The MIT Press), pp. 339-370.

Gunawardena, S., and Goldstein, L. S. (2004). Cargo-carrying motor vehicles on the neuronal highway: transport pathways and neurodegenerative disease. J. Neurobiol. 58, 258-271.

Gundersen, G. G., Kalnoski, M. H., and Bulinski, J. C. (1984). Distinct populations of microtubules: tyrosinated and nontyrosinated alpha tubulin are distributed differently in vivo. Cell 38, 779-789.

Hackney, D. D. (1991). Isolation of kinesin using initial batch ion exchange. Methods Enzymol. 196, 175-181.

Hackney, D. D., Levitt, J. D., and Wagner, D. D. (1991). Characterization of alpha 2 beta 2 and alpha 2 forms of kinesin. Biochem. Biophys. Res. Commun. 174, 810-815.

Hackney, D. D., Levitt, J. D., and Suhan, J. (1992). Kinesin undergoes a 9 S to 6 S conformational transition. J. Biol Chem. 267, 8696-8701.

Hackney, D. D. (1995). Highly processive microtubule-stimulated ATP hydrolysis by dimeric kinesin head domains. Nature 377, 448-450.

Hackney, D. D., and Stock, M. F. (2000). Kinesin's IAK tail domain inhibits initial microtubule-stimulated ADP release. Nat. Cell Biol. 2, 257-260.

Hall, D. H., and Hedgecock, E. M. (1991). Kinesin-related gene unc-104 is required for axonal transport of synaptic vesicles in *C. elegans*. Cell 65, 837-847.

Hancock, W. O., and Howard, J. (1998). Processivity of the motor protein kinesin requires two heads. J. Cell Biol. 140, 1395-1405.

Harrison, B. C., Marchese-Ragona, S. P., Gilbert, S. P., Cheng, N., Steven, A. C., and Johnson, K. A. (1993). Decoration of the microtubule surface by one kinesin head per tubulin heterodimer. Nature 362, 73-75.

Hollenbeck, P. J. (1989). The distribution, abundance and subcellular localization of kinesin. J Cell Biol. 108, 2335-2342.

Hollenbeck, P. J. (1993). Phosphorylation of neuronal kinesin heavy and light chains in vivo. J. Neurochem. 60, 2265-2275.

Horton, A. C., and Ehlers, M. D. (2003). Neuronal polarity and trafficking. Neuron 40, 277-295.

Hua, W., Young, E. C., Fleming, M. L., and Gelles, J. (1997). Coupling of kinesin steps to ATP hydrolysis. Nature 388, 390-393.

Ichihara, K., Kitazawa, H., Iguchi, Y., Hotani, H., and Itoh, T. J. (2001). Visualization of the stop of microtubule depolymerization that occurs at the high-density region of microtubule-associated protein 2 (MAP2). J. Mol. Biol. 312, 107-118.

Inagaki, N., Chihara, K., Arimura, N., Menager, C., Kawano, Y., Matsuo, N., Nishimura, T., Amano, M., and Kaibuchi, K. (2001). CRMP-2 induces axons in cultured hippocampal neurons. Nat. Neurosci. 4, 781-782.

Inoue, S. (1981). Video image processing greatly enhances contrast, quality, and speed in polarization-based microscopy. J. Cell Biol. 89, 346-356.

Jacobson, C., Schnapp, B., and Banker, G.A. (2006) A change in the selective translocation of the Kinesin-1 motor domain marks the initial specification of the axon. Neuron 49, 797-804.

Jareb, M., and Banker, G. (1998). The polarized sorting of membrane proteins expressed in cultured hippocampal neurons using viral vectors. Neuron 20, 855-867.

Jiang, H., and Rao, Y. (2005). Axon formation: fate versus growth. Nat. Neurosci. 8, 544-546.

Junco, A., Bhullar, B., Tarnasky, H. A., and van der Hoorn, F. A. (2001). Kinesin light-chain KLC3 expression in testis is restricted to spermatids. Biol. Reprod. 64, 1320-1330.

Kanaani, J., Diacovo, M. J., El-Husseini Ael, D., Bredt, D. S., and Baekkeskov, S. (2004). Palmitoylation controls trafficking of GAD65 from Golgi membranes to axon-specific endosomes and a Rab5a-dependent pathway to presynaptic clusters. J. Cell Sci.117, 2001-2013.

Kanai, Y., Okada, Y., Tanaka, Y., Harada, A., Terada, S., and Hirokawa, N. (2000). KIF5C, a novel neuronal kinesin enriched in motor neurons. J. Neurosci. 20, 6374-6384.

Kimura, T., Watanabe, H., Iwamatsu, A., and Kaibuchi, K. (2005). Tubulin and CRMP-2 complex is transported via Kinesin-1. J. Neurochem. 93, 1371-1382.

Karcher, R. L., Deacon, S. W., and Gelfand, V. I. (2002). Motor-cargo interactions: the key to transport specificity. Trends Cell Biol. 12, 21-27.

Kikkawa, M., Okada, Y., and Hirokawa, N. (2000). 15 A resolution model of the monomeric kinesin motor, KIF1A. Cell 100, 241-252.

Klopfenstein, D. R., Holleran, E. A., and Vale, R. D. (2002). Kinesin motors and microtubule-based organelle transport in Dictyostelium discoideum. J. Muscle Res. Cell. Motil. 23, 631-638.

Klopfenstein, D. R., Tomishige, M., Stuurman, N., and Vale, R. D. (2002). Role of phosphatidylinositol(4,5)bisphosphate organization in membrane transport by the Unc104 kinesin
motor. Cell 109, 347-358.

Klopfenstein, D. R., and Vale, R. D. (2004). The lipid binding pleckstrin homology domain in UNC-104 kinesin is necessary for synaptic vesicle transport in Caenorhabditis elegans. Mol. Biol. Cell 15, 3729-3739.

Klotz, A., Rutberg, M., Denoulet, P., and Wallin, M. (1999). Polyglutamylation of atlantic cod tubulin: immunochemical localization and possible role in pigment granule transport. Cell Motil. Cytoskeleton 44, 263-273.

Komarova, Y. A., Akhmanova, A. S., Kojima, S., Galjart, N., and Borisy, G. G. (2002). Cytoplasmic linker proteins promote microtubule rescue in vivo. J. Cell Biol. 159, 589-599.

Larcher, J. C., Boucher, D., Lazereg, S., Gros, F., and Denoulet, P. (1996). Interaction of kinesin motor domains with alpha- and beta-tubulin subunits at a tau-independent binding site. Regulation by polyglutamylation. J. Biol. Chem. 271, 22117-22124.

Lawrence, C. J., Dawe, R. K., Christie, K. R., Cleveland, D. W., Dawson, S. C., Endow, S. A., Goldstein, L. S., Goodson, H. V., Hirokawa, N., Howard, J., et al. (2004). A standardized kinesin nomenclature. J. Cell Biol. 167, 19-22.

Lee, J. R., Shin, H., Ko, J., Choi, J., Lee, H., and Kim, E. (2003). Characterization of the movement of the kinesin motor KIF1A in living cultured neurons. J. Biol. Chem. 278, 2624-2629.

Lee, J. R., Shin, H., Choi, J., Ko, J., Kim, S., Lee, H. W., Kim, K., Rho, S. H., Lee, J. H., Song, H. E., et al. (2004). An intramolecular interaction between the FHA domain and a coiled coil negatively regulates the kinesin motor KIF1A. Embo J. 23, 1506-1515.

Ligon, L. A., Shelly, S. S., Tokito, M., and Holzbaur, E. L. (2003). The microtubule plus-end proteins EB1 and dynactin have differential effects on microtubule polymerization. Mol. Biol. Cell 14, 1405-1417.

Mallik, R., and Gross, S. P. (2004). Molecular motors: strategies to get along. Curr. Biol. 14, R971-982.

Mandell, J. W., and Banker, G. A. (1996). A spatial gradient of tau protein phosphorylation in nascent axons. J. Neurosci. 16, 5727-5740.

Mansfield, S.G., and Gordon-Weeks, P.R. (2002). Dynamic post-translational modification of tubulin in rat cerebral cortical neurons extending neurites in culture: effects of taxol. J. Neurocytol. 20, 654-66.

McIntosh, J.R., and Euteneuer, U. (1984). Tubulin hooks as probes for microtubule polarity: an analysis of the method and an evaluation of data on microtubule polarity in the mitotic spindle. J. Cell Biol. 98, 525-33.

McNally, K. P., Buster, D., and McNally, F. J. (2002). Katanin-mediated microtubule severing can be regulated by multiple mechanisms. Cell. Motil. Cytoskeleton 53, 337-349.

Menager, C., Arimura, N., Fukata, Y., and Kaibuchi, K. (2004). PIP3 is involved in neuronal polarization and axon formation. J. Neurochem. 89, 109-118.

Miki, H., Setou, M., Kaneshiro, K., and Hirokawa, N. (2001). All kinesin superfamily protein, KIF, genes in mouse and human. Proc. Natl. Acad. Sci. USA 98, 7004-7011.

Miller, R. H., Lasek, R. J., and Katz, M. J. (1987). Preferred microtubules for vesicle transport in lobster axons. Science 235, 220-222.

Nakata, T., and Hirokawa, N. (2003). Microtubules provide directional cues for polarized axonal transport through interaction with kinesin motor head. J. Cell Biol. 162, 1045-1055.

Nangaku, M., Sato-Yoshitake, R., Okada, Y., Noda, Y., Takemura, R., Yamazaki, H., and Hirokawa, N. (1994). KIF1B, a novel microtubule plus end-directed monomeric motor protein for transport of mitochondria. Cell, 79:1209-20.

Nishimura, T., Kato, K., Yamaguchi, T., Fukata, Y., Ohno, S., and Kaibuchi, K. (2004). Role of the PAR-3-KIF3 complex in the establishment of neuronal polarity. Nat. Cell Biol. 6, 328-334.

Nogales, E., Wolf, S. G., and Downing, K. H. (1998). Structure of the alpha beta tubulin dimer by electron crystallography. Nature 391, 199-203.

Nogales, E. (2000). Structural insights into microtubule function. Annu. Rev. Biochem. 69, 277-302.

Okada, Y., Yamazaki, H., Sekine-Aizawa, Y., and Hirokawa, N. (1995). The neuron-specific kinesin superfamily protein KIF1A is a unique monomeric motor for anterograde axonal transport of synaptic vesicle precursors. Cell 81, 769-780.

Okada, Y., and Hirokawa, N. (1999). A processive single-headed motor: kinesin superfamily protein KIF1A. Science 283, 1152-1157.

Okada, Y., and Hirokawa, N. (2000). Mechanism of the single-headed processivity: diffusional anchoring between the K-loop of kinesin and the C terminus of tubulin. Proc. Natl. Acad. Sci. USA 97, 640-645.

Otsuka, A. J., Jeyaprakash, A., Garcia-Anoveros, J., Tang, L. Z., Fisk, G., Hartshorne, T., Franco, R., and Born, T. (1991). The C. elegans unc-104 gene encodes a putative kinesin heavy chain-like protein. Neuron 6, 113-122.

Pierce, D. W., Hom-Booher, N., Otsuka, A. J., and Vale, R. D. (1999). Single-molecule behavior of monomeric and heteromeric kinesins. Biochemistry 38, 5412-5421.

Qiang, L., Yu, W., Andreadis, A., Luo, M., and Baas, P. W. (2006). Tau protects microtubules in the axon from severing by katanin. J. Neurosci. 26, 3120-3129.

Rahman, A., Friedman, D. S., and Goldstein, L. S. (1998). Two kinesin light chain genes in mice. Identification and characterization of the encoded proteins. J. Biol. Chem. 273, 15395-15403.

Redeker, V., Levilliers, N., Vinolo, E., Rossier, J., Jaillard, D., Burnette, D., Gaertig, J., and Bre, M. H. (2005). Mutations of tubulin glycylation sites reveal cross-talk between the C termini of alpha- and beta-tubulin and affect the ciliary matrix in Tetrahymena. J. Biol.Chem. 280, 596-606.

Reynolds, C. H., Utton, M. A., Gibb, G. M., Yates, A., and Anderton, B. H. (1997). Stress-activated protein kinase/c-jun N-terminal kinase phosphorylates tau protein. J. Neurochem. 68, 1736-1744.

Rogers, S. L., Rogers, G. C., Sharp, D. J., and Vale, R. D. (2002). Drosophila EB1 is important for proper assembly, dynamics, and positioning of the mitotic spindle. J. Cell Biol. 158, 873-884.

Rosenbaum, J. (2000). Cytoskeleton: functions for tubulin modifications at last. Curr. Biol. 10,
R801-803.

Sampo, B., Kaech, S., Kunz, S., and Banker, G. (2003). Two distinct mechanisms target membrane proteins to the axonal surface. Neuron 37, 611-624.

Samsonov, A., Yu, J. Z., Rasenick, M., and Popov, S. V. (2004). Tau interaction with microtubules in vivo. J. Cell Sci. 117, 6129-6141.

Schnapp, B. J., Vale, R. D., Sheetz, M. P., and Reese, T. S. (1985). Single microtubules from squid axoplasm support bidirectional movement of organelles. Cell 40, 455-462.

Schnapp, B. J. (2003). Trafficking of signaling modules by kinesin motors. J. Cell Sci. 116, 2125-2135.

Schnitzer, M. J., and Block, S. M. (1997). Kinesin hydrolyses one ATP per 8-nm step. Nature 388, 386-390.

Scholey, J. M. (2003). Intraflagellar transport. Annu. Rev. Cell Dev. Biol. 19, 423-443.

Schwamborn, J. C., and Puschel, A. W. (2004). The sequential activity of the GTPases Rap1B and Cdc42 determines neuronal polarity. Nat. Neurosci. 7, 923-929.

Seitz, A., Kojima, H., Oiwa, K., Mandelkow, E. M., Song, Y. H., and Mandelkow, E. (2002). Single-molecule investigation of the interference between kinesin, tau and MAP2c. Embo J. 21, 4896-4905.

Setou, M., Seog, D. H., Tanaka, Y., Kanai, Y., Takei, Y., Kawagishi, M., and Hirokawa, N. (2002). Glutamate-receptor-interacting protein GRIP1 directly steers kinesin to dendrites. Nature 417, 83-87.

Shi, S. H., Jan, L. Y., and Jan, Y. N. (2003). Hippocampal neuronal polarity specified by spatially localized mPar3/mPar6 and PI 3-kinase activity. Cell 112, 63-75.

Silverman, M. A., Kaech, S., Jareb, M., Burack, M. A., Vogt, L., Sonderegger, P., and Banker, G. (2001). Sorting and directed transport of membrane proteins during development of hippocampal neurons in culture. Proc. Natl. Acad. Sci. USA 98, 7051-7057.

Simons, M., Ikonen, E., Tienari, P. J., Cid-Arregui, A., Monning, U., Beyreuther, K., and Dotti, C. G. (1995). Intracellular routing of human amyloid protein precursor: axonal delivery followed by transport to the dendrites. J. Neurosci. Res. 41, 121-128.

Song, Y. H., and Mandelkow, E. (1993). Recombinant kinesin motor domain binds to beta-tubulin and decorates microtubules with a B surface lattice. Proc. Natl. Acad. Sci. USA 90, 1671-1675.

Stepanova, T., Slemmer, J., Hoogenraad, C. C., Lansbergen, G., Dortland, B., De Zeeuw, C. I., Grosveld, F., van Cappellen, G., Akhmanova, A., and Galjart, N. (2003). *Visualization of microtubule growth in cultured neurons via the use of EB3-GFP (end-*binding protein 3-green fluorescent protein). J. Neurosci. 23, 2655-2664.

Stock, M. F., Guerrero, J., Cobb, B., Eggers, C. T., Huang, T. G., Li, X., and Hackney, D. D. (1999). Formation of the compact confomer of kinesin requires a COOH-terminal heavy chain domain and inhibits microtubule-stimulated ATPase activity. J. Biol. Chem. 274, 14617-14623.

Svoboda, K., Schmidt, C. F., Schnapp, B. J., and Block, S. M. (1993). Direct observation of kinesin stepping by optical trapping interferometry. Nature 365, 721-727.

Tanaka, Y., Kanai, Y., Okada, Y., Nonaka, S., Takeda, S., Harada, A., and Hirokawa, N. (1998).
Targeted disruption of mouse conventional kinesin heavy chain, kif5B, results in abnormal perinuclear clustering of mitochondria. Cell 93, 1147-1158.

Thorn, K.S., Ubersax, J.A., and Vale, R.D.. (2000). Engineering the processive run length of the kinesin motor. J. Cell Biol. 151:1093-100.

Tirnauer, J. S., Grego, S., Salmon, E. D., and Mitchison, T. J. (2002). EB1-microtubule interactions in Xenopus egg extracts: role of EB1 in microtubule stabilization and mechanisms of targeting to microtubules. Mol. Biol. Cell 13, 3614-3626.

Tomishige, M., Klopfenstein, D. R., and Vale, R. D. (2002). Conversion of Unc104/KIF1A kinesin into a processive motor after dimerization. Science 297, 2263-2267.

Trinczek, B., Ebneth, A., Mandelkow, E. M., and Mandelkow, E. (1999). Tau regulates the attachment/detachment but not the speed of motors in microtubule-dependent transport of single vesicles and organelles. J. Cell Sci. 112, 2355-2367.

Tsai, M. Y., Morfini, G., Szebenyi, G., and Brady, S.T. (2000). Release of kinesin from vesicles by hsc70 and regulation of fast axonal transport. Mol. Biol. Cell 11, 2161-73.

Vale, R. D., Reese, T. S., and Sheetz, M. P. (1985a). Identification of a novel force-generating protein, kinesin, involved in microtubule-based motility. Cell 42, 39-50.

Vale, R. D., Schnapp, B. J., Reese, T. S., and Sheetz, M. P. (1985b). Organelle, bead, and microtubule translocations promoted by soluble factors from the squid giant axon. Cell 40, 559-569.

Vale, R. D., Funatsu, T., Pierce, D. W., Romberg, L., Harada, Y., and Yanagida, T. (1996). Direct observation of single kinesin molecules moving along microtubules. Nature 380, 451-453.

Vale, R. D., and Fletterick, R. J. (1997). The design plan of kinesin motors. Annu. Rev. Cell Dev. Biol. 13, 745-777.

Vale, R. D., and Milligan, R. A. (2000). The way things move: looking under the hood of molecular motor proteins. Science 288, 88-95.

Vale, R. D. (2003). The molecular motor toolbox for intracellular transport. Cell 112, 467-480.

Vaughan, K. T. (2004). Surfing, regulating and capturing: are all microtubule-tip-tracking proteins created equal? Trends Cell Biol. 14, 491-496.

Vaughan, K. T. (2005). TIP maker and TIP marker; EB1 as a master controller of microtubule plus ends. J. Cell Biol. 171, 197-200.

Verhey, K. J., Lizotte, D. L., Abramson, T., Barenboim, L., Schnapp, B. J., and Rapoport, T. A. (1998). Light chain-dependent regulation of Kinesin's interaction with microtubules. J. Cell Biol. 143, 1053-1066.

Verhey, K. J., Meyer, D., Deehan, R., Blenis, J., Schnapp, B. J., Rapoport, T. A., and Margolis, B. (2001). Cargo of kinesin identified as JIP scaffolding proteins and associated signaling molecules. J. Cell Biol. 152, 959-970.

West, A. E., Neve, R. L., and Buckley, K. M. (1997). Identification of a somatodendritic targeting signal in the cytoplasmic domain of the transferrin receptor. J. Neurosci. 17, 6038-6047.

Westermann, S., and Weber, K. (2003) Post-translational modifications regulate microtubule function. Nat. Rev. Mol. Cell. Biol. 4:938-47.

Wiggin, G. R., Fawcett, J. P., and Pawson, T. (2005). Polarity proteins in axon specification and synaptogenesis. Dev. Cell 8, 803-816.

Xia, C., Rahman, A., Yang, Z., and Goldstein, L. S. (1998). Chromosomal localization reveals three kinesin heavy chain genes in mouse. Genomics 52, 209-213.

Xia, C. H., Roberts, E. A., Her, L. S., Liu, X., Williams, D. S., Cleveland, D. W., and Goldstein, L. S. (2003). Abnormal neurofilament transport caused by targeted disruption of neuronal kinesin heavy chain KIF5A. J. Cell Biol. 161, 55-66.

Yildiz, A., Forkey, J. N., McKinney, S. A., Ha, T., Goldman, Y. E., and Selvin, P. R. (2003). Myosin V walks hand-over-hand: single fluorophore imaging with 1.5-nm localization. Science 300, 2061-2065.

Yildiz, A., Tomishige, M., Vale, R. D., and Selvin, P. R. (2004). Kinesin walks hand-over-hand. Science 303, 676-678.

Yonekawa, Y., Harada, A., Okada, Y., Funakoshi, T., Kanai, Y., Takei, Y., Terada, S., Noda, T., and Hirokawa, N. (1998). Defect in synaptic vesicle precursor transport and neuronal cell death in KIF1A motor protein-deficient mice. J. Cell Biol. 141, 431-441.

Yonekawa, Y., Harada, A., Okada, Y., Funakoshi, T., Kanai, Y., Takei, Y., Terada, S., Noda, T., and Hirokawa, N. (1998). Defect in synaptic vesicle precursor transport and neuronal cell death in KIF1A motor protein-deficient mice. J. Cell Biol. 141, 431-441.

Zhou, H. M., Brust-Mascher, I., and Scholey, J. M. (2001). Direct visualization of the movement of the monomeric axonal transport motor UNC-104 along neuronal processes in living Caenorhabditis elegans. J. Neurosci. 21, 3749-3755.